Modern Pathology (2004) 17, 423–429

www.modernpathology.org

# Diagnostic importance of CD179a/b as markers of precursor B-cell lymphoblastic lymphoma

Nobutaka Kiyokawa[1], Takaomi Sekino[1], Tsubasa Matsui[1], Hisami Takenouchi[1], Kenichi Mimori[1], Wei-ran Tang[1], Jun Matsui[1], Tomoko Taguchi[1], Yohko U Katagiri[1], Hajime Okita[1], Yoshinobu Matsuo[2], Hajime Karasuyama[3] and Junichiro Fujimoto[1]

[1]*Department of Developmental Biology, National Research Institute for Child Health and Development, Japan;* [2]*Fujisaki Cell Center, Hayashibara Biochemical Labs Inc, Okayama, Japan and* [3]*Department of Immune Regulation, Tokyo Medical and Dental University, Graduate School of Medicine, Tokyo, Japan*

**Surrogate light chains consisting of VpreB (CD179a) and λ5 (CD179b) are expressed in precursor B cells lacking a complete form of immunoglobulin and are thought to act as substitutes for conventional light chains. Upon differentiation to immature and mature B cells, CD179a/b disappear and are replaced with conventional light chains. Thus, these molecules may be useful as essential markers of precursor B cells. To examine the expression of the surrogate light-chain components CD179a and CD179b in precursor B-cell lymphoblastic lymphoma, we analyzed tissue sections using immunohistochemistry techniques. Among a number of monoclonal antibodies for the surrogate light chains, VpreB8 and SL11 were found to detect CD179a and CD179b, respectively, in acetone-fixed fresh frozen sections. Moreover, we also observed VpreB8 staining in formalin-fixed, paraffin-embedded sections. Using these antibodies, we found that CD179a/b were specifically expressed in precursor B-cell lymphoblastic lymphomas, but not in mature B-cell lymphomas in childhood. Furthermore, other pediatric tumors that must be included in a differential diagnosis of precursor B-cell lymphoblastic lymphoma, including precursor T-cell lymphoblastic lymphoma, extramedullary myeloid tumors, and Ewing sarcoma, were also negative for both CD179a and CD179b. Our data indicate that CD179a and CD179b may be important markers for the immunophenotypic diagnosis of precursor B-cell lymphoblastic lymphomas.**
*Modern Pathology* (2004) **17**, 423–429, advance online publication, 20 February 2004; doi:10.1038/modpathol.3800079

**Keywords:** CD179a/b; lymphoblastic lymphoma; precursor B cells; immunohistochemistry; diagnosis

B cells are characterized by the surface expression of immunoglobulin (Ig), consisting of a heavy chain (HC) and conventional κ or λ light chains (LCs). The Ig expressed in B cells is associated with the Igα/Igβ (CD79a/b) complex and forms a B-cell antigen receptor complex. In contrast to these mature B cells, precursor B cells do not express Ig, although they do contain Ig-related components. For example, more primitive pro-B cells already express the Igα/Igβ complex and contain surrogate LCs, consisting of VpreB (CD179a) and λ5 (CD179b).[1–5] Through the successful rearrangement of HC genes, pro-B cells undergo differentiation into pre-B cells and start to express a premature antigen receptor, namely the pre-B-cell receptor (pre-BCR), consisting of μ HC, CD179a/b and the Igα/Igβ heterodimer.[6–9] Upon further differentiation from pre-B cells to B cells, CD179a/b disappear and are replaced with conventional LC.

The stage-specific developmental expression of Ig-related molecules is an essential characteristic of B-lineage cells and is conserved not only in normal cells but also in neoplastic cells of B lineage. Indeed, precursor B acute lymphoblastic leukemias (ALL), which originate from precursor B cells and lack the complete form of Ig, are known to express CD179a/b, while mature and Ig-expressing B-cell ALLs do not.[10] Precursor B-cell lymphoblastic lymphoma (B-LBL) is a disease in which neoplastic precursor B cells proliferate without the obvious involvement of blood or bone marrow and thus exhibits immunophenotypic characteristics that are similar to those of precursor B-ALL.[11,12] Neoplasms of precursor B cells most commonly present as a form of ALL during childhood, and the presentation of B-LBL is infrequent, but may occur in patients of any

Correspondence: N Kiyokawa, MD, PhD, Department of Developmental Biology, National Research Institute for Child Health and Development, 3-35-31, Taishido, Setagaya-ku, Tokyo 154-8567, Japan.
E-mail: nkiyokawa@nch.go.jp
Received 21 August 2003; revised 26 November 2003; accepted 26 December 2003; published online 20 February 2004

age, frequently involving the skin, bone, or lymph nodes. Owing to the rareness of B-LBL and its morphological and immunophenotypic similarities to mature B-cell lymphomas in some cases, distinguishing between these diseases is of great importance, especially in the field of pediatric oncology, because the treatment strategies for these two diseases are quite different. In addition, other tumors, including precursor T-cell lymphoblastic lymphoma (T-LBL), extramedullary myeloid tumors, and Ewing sarcoma, must also be included in a differential diagnosis of B-LBL.

In an attempt to characterize B-LBL using the expression of Ig-related molecules and to examine the utility of such a method for diagnosis, we examined CD179a/b expression in B-LBL tissues using immunohistochemistry. CD179a/b was found to be specifically expressed in B-LBL, but not in mature B-cell lymphomas and other tumors in childhood. The usefulness of CD179a/b as diagnostic markers for B-LBL is discussed.

## Materials and methods

### Materials

The human pre-B-cell line HPB-NULL[10] and the Burkitt cell line Ramos (Japanese Cancer Research Resources Bank, Tokyo, Japan) were used in this study. Cells were maintained in RPMI1640 supplemented with 10% fetal calf serum at 37°C in a humidified 5% $CO_2$ atmosphere.

Biopsy specimens from pediatric patients, including 11 patients with B-LBL, seven patients with Burkitt lymphoma, three patients with diffuse large B-cell lymphoma, seven patients with T-LBL, three patients with extramedullary myeloid tumors, and three patients with Ewing sarcoma, were selected from medical files collected between 1985 and 2003 at the Department of Developmental Biology, National Research Institute for Child Health and Development. In each case, the initial diagnosis was based on morphological observations of hematoxylin and eosin (H&E)-stained, formalin-fixed, paraffin-embedded tissues, the immunophenotypic characteristics revealed by immunohistochemistry using acetone-fixed, fresh frozen sections, and the patient's clinical features. In some cases, immunophenotyping was also performed using flow cytometric analysis of a single-cell suspension prepared from the tissue. To examine CD179a/b expression, snap-frozen tissues in OCT compounds stored at −85°C after the initial diagnosis were used.

The following mouse monoclonal antibodies (mAbs) were used in this study: anti-CD179a (HSL96), anti-CD179b (HSL11), anti-conformational pre-BCR (HSL2),[10] anti-CD20 (L26),[13] anti-HLA-DR,[14] and anti-CD10 (IF6).[15] HSL2 is a unique mAb that does not bind to each component of the pre-BCR, but recognizes a conformational epitope formed only when the $\mu$ HC and CD179a/b surrogate LC associate with each other to make the pre-BCR complex.[10] In addition, several commercially available mAbs were also used: anti-$\mu$ (G20-127), anti-CD179a (VpreB8 and VpreB9), and anti-CD19 (Leu12) from BD Pharmingen (San Diego, CA, USA); anti-$\kappa$ (HP6053) and anti-$\lambda$ (HP6054) from Zymed Laboratories Inc. (San Francisco, CA, USA); anti-CD79a (HM-57), anti-CD22 (4KB128), and anti-TdT (HT-1/3/4) from DAKO (Glostrup, Denmark); anti-CD179a (4G7) from Coulter/Immunotech Inc. (Westbrook, MA, USA); anti-TdT (SEN28) from Nichirei Co. (Tokyo, Japan); and anti-CD179a (B-MAD-688) from Biocarta (San Diego, CA, USA). The anti-CD77 (1A4) used in this study was a generous gift from Dr S Hakomori of the University of Washington, Seattle, WA, USA and Otsuka Assay Laboratories, Kawauchi-cho, Tokushima, Japan. Secondary Abs, including fluorescence- and enzyme-conjugated Abs, were purchased from Jackson Laboratory, Inc., West Grove, PA, USA.

### Flow Cytometry

The cells were stained with mAbs and analyzed by flow cytometry (EPICS-XL, Coulter) as described previously.[15] Cytoplasmic antigens were stained using CytoStain™ Kits (BD Pharmingen), according to the manufacturer's protocol.

### Immunohistochemistry

Immunohistochemical staining of acetone-fixed fresh frozen sections was performed as described elsewhere.[16] Briefly, fresh frozen sections from each tissue were prepared using a cryostat apparatus and fixed in acetone for 15 min at 4°C. After washing in phosphate-buffered saline (PBS) and blocking with normal rabbit serum, the sections were incubated with mAbs at appropriate dilutions for 30 min at room temperature. Sections were then washed with PBS and incubated with horseradish peroxidase (HRP)-conjugated rabbit anti-mouse antibodies for 30 min at room temperature. After washing with PBS, color development was performed in diaminobenzidine solution (10 mM in 0.05 M Tris-HCl, pH 7.5) with 0.003% $H_2O_2$.

For the cell line samples, the cells were cytocentrifuged on slide glasses using Cytospin III (Shandon Scientific Ltd., Pittsburgh, PA, USA). After fixation with acetone, immunohistochemical staining was performed as described above. In addition, other fixatives, including paraformaldehyde and Zamboni's fixative, were also tested.

The formalin-fixed, paraffin-embedded tissue specimens were initially deparaffinized and then treated using the heat-induced epitope retrieval method in 10 mM of citrate buffer, pH 6.0; immunohistochemical staining was performed using the CSA system (DAKO) according to the manufacturer's protocol.

## Results

### Immunohistochemical Staining of CD179a/b in Acetone-fixed Cytocentrifuged Cell Lines

As reported previously and presented in Figure 1, the mAbs HSL96, HSL11, and HSL2 recognized CD179a/VpreB, CD179b/λ5, and conformational pre-BCR, respectively, in membrane-permeabilized cells when analyzed using flow cytometry.[10] We first examined whether these mAbs could also be used for immunohistochemical staining in acetone-fixed cells. When acetone-fixed, cytocentrifuged pre-B-ALL HPB-NULL cells expressing conformational pre-BCR were tested, the HSL11 mAb was able to detect CD179b at a concentration of 5 μg/ml; neither the HSL96 nor the HSL2 mAbs detected this molecule (Figure 1). Typically, a cytoplasmic staining pattern was observed in HPB-NULL cells using HSL11. In contrast, HSL11 did not react with similarly treated Ramos Burkitt cells, which express the complete form of Ig (μλ), but lack the surrogate LCs, suggesting that CD179b binds specifically to SL11.

We also examined the staining patterns produced by commercially available anti-CD179a mAbs: VpreB8, VpreB9, 4G7, and B-MAD-688. When these four anti-CD179a mAbs were examined, only the VpreB8 mAb reacted with CD179a in acetone-fixed HPB-NULL cells (data not shown). However, VpreB8 mAb exhibited a weak nonspecific binding with the nuclei of acetone-fixed Ramos cells at high mAb concentrations. A concentration of 1.25 μg/ml was optimized as a sufficient and specific condition for CD179a detection in precursor B-ALL cells, which does not produce a nonspecific reaction in Burkitt cells (data not shown).

We further examined whether SL11 and VpreB8 could be used for immunohistochemical staining in cells treated with other fixatives and observed that both mAbs react with Zamboni's fixative-treated cells, but not with paraformaldehyde-treated cells (data not shown).

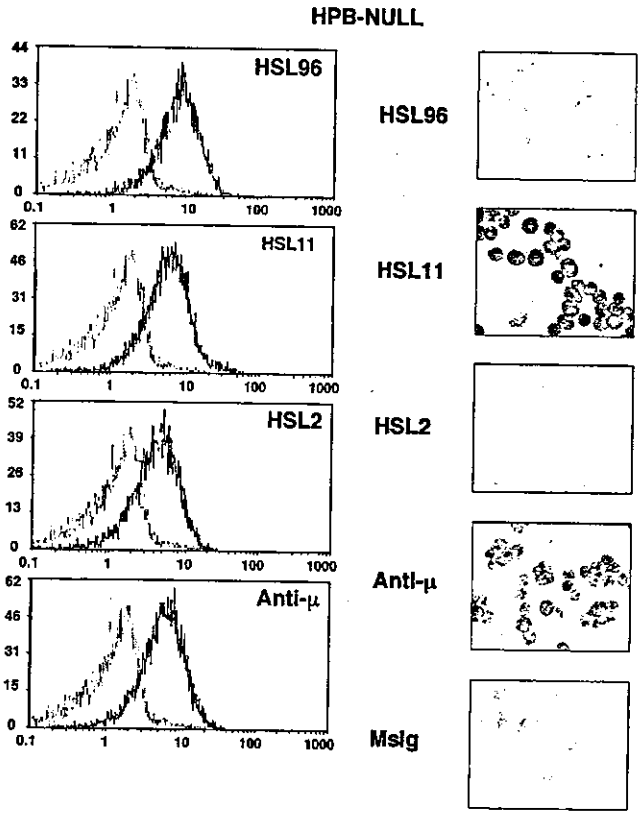


**Figure 1** Immunohistochemical detection of CD179b by HSL11 in acetone-fixed, cytocentrifuged precursor B-ALL cell lines. Pre-BCR-expressing HPB-NULL cells were permeabilized and stained with specific mAbs, as indicated, and analyzed using flow cytometry (left panels). The resulting histograms (solid lines) were superimposed on those of the negative control (cells stained with isotype-matched control mouse Ig, broken light lines) and displayed. *X*-axis, fluorescence intensity; *Y*-axis, relative cell number. In parallel, HPB-NULL cells were cytocentrifuged, acetone-fixed, and stained with each mAb, as indicated, using immunohistostaining (right panels). HSL11 is strongly positive and anti-μ is moderately positive, but others are negative. MsIg, iso-type matched control mouse immunoglobulin.

### Immunohistochemical Staining of CD179a/b in Acetone-fixed Fresh Frozen Tissues

Next, we used immunohistochemistry to examine whether VpreB8 and HSL11 could detect CD179a/b in clinical childhood B-LBL specimens. When acetone-fixed fresh frozen sections prepared from biopsy specimens obtained from B-LBL patients were examined using immunohistochemical staining, both VpreB8 and HSL11 were found to react with the tissues (Figure 2 and Table 1). Typically, a diffuse cytoplasmic staining pattern was observed in B-LBL tissues using both mAbs (Figure 2). Cases were considered as positive if most of the blasts present in the tissue were clearly stained. As summarized in Table 1, nine out of 10 (90%) B-LBL patients and eight out of 11 (73%) B-LBL patients were positive for VpreB8 and HSL11, respectively. In contrast, no positive staining for VpreB8 or HSL11 was seen in either the Burkitt lymphoma tissues (seven cases) or the diffuse large B-cell lymphoma tissues (three cases), suggesting that both VpreB8 and HSL11 react specifically with B-LBL cells, but not with mature B-cell lymphomas in childhood.

We also examined the other pediatric tumors that must also be included in a differential diagnosis of B-LBL. As presented in Table 2, when acetone-fixed fresh frozen sections prepared from biopsy specimens obtained from seven T-LBL cases, three extramedullary myeloid tumors, and two Ewing sarcoma cases were examined similarly, all of these cases were negative for both VpreB8 and HSL11, indicating the specificity of these mAbs to B-LBL cells.

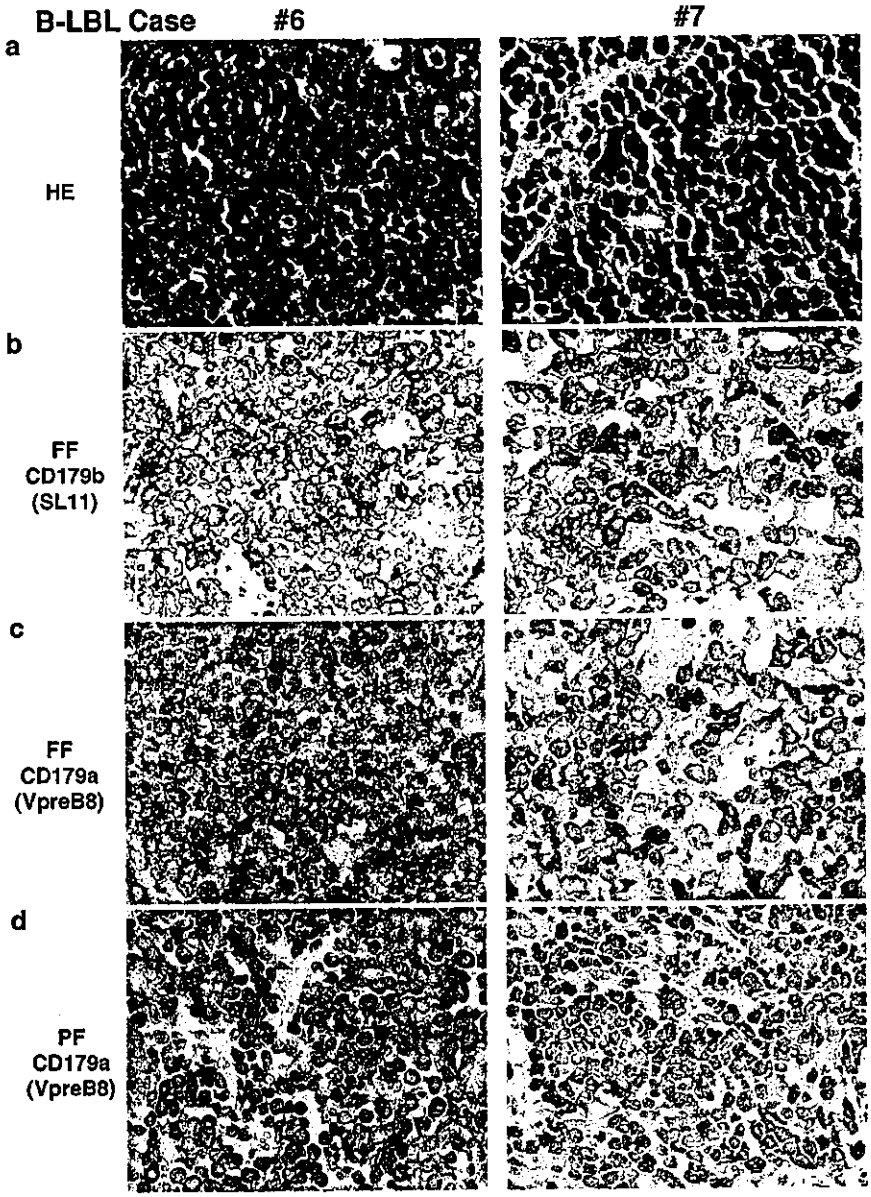


**Figure 2** Immunohistochemical detection of CD179a and CD179b. CD179a and CD179b were detected in B-lymphoblastic lymphoma tissues using immunohistochemical staining on acetone-fixed fresh frozen sections ((**b**), (**c**), FF) and formalin-fixed, paraffin-embedded tissue sections ((**d**), PF) from biopsy tissues. The H&E-staining of formalin-fixed and paraffin-embdded tissues is also shown ((**a**), HE).

### Immunohistochemical Staining of CD179a in Formalin-fixed, Paraffin-embedded Tissues

Next, we examined whether mAbs against CD179a and CD179b could be used in formalin-fixed, paraffin-embedded tissues. When paraffin-embedded tissues prepared from clinical specimens obtained from B-LBL patients were examined using immunohistochemical staining with the heat-induced epitope retrieval treatment, only VpreB8 reacted with the tissue. The staining results were consistent with those obtained from the immunostaining of acetone-fixed frozen sections. None of the other mAbs reacted with the B-LBL samples. Since higher concentrations of VpreB8 resulted in nonspecific nuclear staining in paraffin sections of Burkitt lymphomas, care must be taken when deciding the appropriate conditions for the use of this mAb.

## Discussion

In the current study, we clearly presented that both VpreB8 and HSL11 are useful for the immunohistochemical detection of CD179a and CD179b, respectively, in acetone-fixed B-LBL tissues. Furthermore, VpreB8 can also be used in paraffin-embedded sections. The reactivities of these Abs were highly specific for B-LBL. Reactivity was not seen in tissues of Burkitt lymphoma, diffuse large B-cell

**Table 1** Detection of CD179a and CD179b in B-lineage lymphoma tissues using immunohistochemical staining in acetone-fixed fresh frozen sections

| *Case no.* | *Age (years)* | *Sex* | *Origin* | *CD179a* | *CD179b* | *TdT* | *CD34* | *CD19* | *CD79a* | *DR* | *CD20* | *μ* | *LC* | *CD10* | *CD77* |
|---|---|---|---|---|---|---|---|---|---|---|---|---|---|---|---|
| *B-LBL* | | | | | | | | | | | | | | | |
| 1 | 4 | M | Bil-CL | + | + | + | − | + | + | + | +P | − | − | + | − |
| 2[a] | 9 | M | R-testis | + | + | + | − | + | + | + | +M | NT | NT | + | − |
| 3 | 7 | M | L-CL | + | + | + | − | + | + | + | − | + | − | + | − |
| 4 | 5 | F | L-CL | + | + | + | − | + | + | + | − | − | − | + | − |
| 5 | 7 | F | L-CL | + | + | + | + | + | + | + | − | + | − | + | − |
| 6 | 1 | F | R-CL | + | + | + | − | + | + | + | − | − | − | + | − |
| 7 | 12 | M | AT | + | + | − | − | + | + | + | − | − | − | + | − |
| 8 | 5 | F | L-upper arm | + | − | − | − | + | + | + | +M | − | − | + | NT |
| 9 | 7 | M | L-CL | − | − | + | − | + | + | + | +P | − | − | + | NT |
| 10 | 4 | F | R-radius | + | − | − | + | + | + | + | − | − | − | + | − |
| 11 | 9 | M | CNS | NT | + | + | NT | + | + | NT | NT | + | NT | NT | NT |
| *Burkitt* | | | | | | | | | | | | | | | |
| 1 | 6 | F | AT | − | − | − | − | + | + | + | + | + | − | − | + |
| 2 | 7 | M | AT | − | − | − | − | + | + | + | + | + | Lamda | + | + |
| 3 | 15 | M | AT | − | − | − | − | + | + | + | + | + | Lamda | + | + |
| 4 | 4 | M | AT | − | − | − | − | + | + | + | + | + | Kappa | + | + |
| 5 | 6 | M | AT | − | − | − | − | + | + | + | + | + | Kappa | + | − |
| 6 | 5 | M | AT | − | − | − | − | + | + | + | + | + | Kappa | + | + |
| 7 | 4 | M | AT | − | − | − | − | + | + | + | + | + | Lamda | + | + |
| *B-DL* | | | | | | | | | | | | | | | |
| 1 | 7 | F | R-CL | − | − | − | − | + | + | + | + | + | Lamda | − | − |
| 2 | 6 | M | AT | − | − | − | − | + | + | + | + | + | Lamda | − | − |
| 3 | 8 | M | R-CL | − | − | − | − | + | + | + | + | + | Lamda | + | − |

B-LBL, precursor B-cell lymphoblastic lymphoma; DL, diffuse large cell lymphoma; Bil, bilateral; L, left; R, right; CL, cervical lymph nodes; AT, abdominal tumor; LC, light chains; NT, not tested; P, patchy staining pattern; M, membranous staining pattern.
[a]Testicular relapse of precursor B acute lymphoblastic leukemia.

**Table 2** Immunohistochemical staining of CD179a and CD179b on acetone-fixed fresh frozen sections of non-B-cell lineage neoplasm tissues

| | *Positivity* | |
|---|---|---|
| | *CD179a* | *CD179b* |
| T-LBL | 0/7 | 0/7 |
| Extramedullary myeloid tumors | | |
| Granulocytic sarcoma | 0/2 | 0/2 |
| AMoL, skin infiltration | 0/1 | 0/1 |
| Ewing sarcoma | 0/2 | 0/2 |

T-LBL, precursor T-cell lymphoblastic lymphoma; AMoL, acute monocytic leukemia.

lymphoma, T-LBL, extramedullary myeloid tumors, and Ewing sarcoma.

In pediatrics, the three major types of B-cell lymphoma are B-LBL, Burkitt lymphoma, and diffuse large B-cell lymphoma; the latter two types must be distinguished from B-LBL since the therapeutic protocols for these diseases are quite different from that for B-LBL. In the Berlin Frankfurt Munster (BFM) study group, for example, B-LBL cases were treated using ALL-type protocol with a total therapy duration of at least 24 months.[17] In contrast, mature B-cell lymphoma cases, including Burkitt lymphoma and diffuse large B-cell lymphoma, are treated using a short course of treatment that is usually completed within a year.[18] Each type of B-lineage lymphoma is morphologically unique and distinctive upon histological examination. In the practical pathological diagnosis of lymphomas, however, pathologists may experience difficulties in differentiating B-LBL from other B-lineage lymphomas, especially when only poor-quality biopsy specimens are available.[12] Unfortunately, pathologists are not always familiar with B-LBL because of its rarity among childhood lymphomas; as a result, patients with B-LBL may be misdiagnosed as having mature B-cell lymphoma, such as Burkitt lymphoma. The similarity in marker expression patterns for B-LBL and Burkitt lymphoma is also partly responsible for the risk of misdiagnosis.[11,12]

TdT is considered to be a reliable marker for the diagnosis of cases of precursor lymphocyte origin,[11,12] but TdT is not always positive in B-LBL cases as reported by several different groups.[19–22] For example, Mertelsmann *et al*[20] reported that TdT was absent in approximately 5% of ALL and LBL cases. Orazi *et al*[21] also reported that 6% (two out of 35) of LBL cases was TdT-negative assessed by immunohistochemical staining. On the other hand, CD34 is expressed on human bone marrow progenitor cells and leukemic blasts, and is considered to be an immature marker. Although the expression of CD34 on B-lineage lymphomas suggests their precursor B-cell origin, the positivity of CD34 among the B-LBL cases is approximately 50%. In addition, both TdT

and CD34 are not restricted to the precursor of B cells. In contrast, CD20 is a B-cell-specific marker and its expression increases with B-cell maturation. Therefore, the absence of CD20 expression in B-lineage lymphomas suggests their precursor B-cell origin. However, CD20 expression is variable among cases of B-LBL and approximately 50% of B-LBL cases are CD20-positive, exhibiting sometimes a strong membranous staining pattern.[11] Therefore, it is difficult to specify a B-precursor origin using CD20 expression alone. Based on the above evidences, the development of other markers capable of revealing a precursor B-cell origin is urgently required; in this regard, the results described here are expected to assist in the proper diagnosis of B-LBL among B-cell lymphomas in childhood.

CD179a and CD179b are essential for the development of precursor B cells. Although their biological significance is not fully understood, they are believed to serve as surrogate LCs expressed with $\mu$ HCs in pre-BCR to determine whether the clone should survive or die. After subsequent rearrangements in $\kappa$ or $\lambda$ LC genes, the expression of the surrogate LCs is suppressed.[6–9] The utilization of such functional molecules in the diagnosis of precursor B-cell lymphomas is appropriate if the expression is conserved even in tumor cells. In precursor B-ALL cells, we previously reported that CD179a, CD179b, and the complete form of pre-BCR were detected by HSL96, HSL11, and HSL2, respectively, and were expressed in most of the CD10-positive precursor B-ALL cases,[10] suggesting that these markers may be useful for the further classification of this disease. Consistent with this observation, CD179a and CD179b, detected by VpreB8 and HSL11, respectively, were frequently expressed in B-LBL cases, whose origin is comparable to that of precursor B-ALL. Thus, the successful employment of these functional molecules in the diagnosis of B-cell lymphomas is another important aspect emphasized in this study.

As shown here, CD179a and CD179b immunohistochemistry can identify more than 90% of B-LBL cases. In our series, the positivity of TdT among the B-LBL cases examined was lower (73%) than that of previous reports.[19–22] The reason for this discrepancy is not known, but it is noteworthy that three TdT-negative cases were positive for either CD179a or CD179b or both. Thus, by combining the TdT and CD179 markers, we believe that virtually all B-LBL cases can be properly judged as having a precursor B-cell origin. The absence of CD179a/b reactivity in Burkitt and diffuse large B-cell-type lymphomas further supports the reliability of this marker.

Occasionally, B-LBL may be misdiagnosed as Ewing sarcoma, since these two diseases have similar morphologies and immunostaining patterns.[23] CD99 (MIC2) was previously considered to be a specific marker for Ewing sarcoma, but this molecule has now been shown to be frequently expressed in B-LBL. Bone tumors with a blastic morphology and a CD45−, CD20−, MIC2+ phenotype can be diagnosed as Ewing sarcoma. In such cases, immunostaining for CD179a/b along with TdT and CD79a will lead to a proper diagnosis. In addition, immunostaining for CD179a/b is also useful for distinguishing B-LBL from either T-LBL or extramedullary myeloid tumors, both of which are included in frequent differential for B-LBL.

Diagnostic markers must be usable in paraffin sections for practical diagnostic procedures. In this regard, the utilization of mAb VpreB8 in paraffin sections, as demonstrated in this report, should facilitate its use in daily diagnostics. Caution must be exercised, however, when using VpreB8 because this antibody may produce nonspecific binding. After careful examination, we selected a concentration of 1.25 $\mu$g/ml for our system; however, this value should be evaluated for each laboratory in which the mAb is used, since differences in detection systems may affect the results. Other than VpreB8, unfortunately, none of the mAbs against CD179a/b tested in this study was useful for immunohistochemical detection in paraffin-embedded sections. Since the expression of CD179b was always accompanied by that of CD179a in our cases assessed using fresh frozen section staining (Table 1), paraffin section staining with VpreB8 may be sufficient for the diagnosis of B-LBL. However, the generation of novel mAbs against CD179a/b and preBCR that can react in paraffin sections would be useful and may provide more convincing results.

In conclusion, we have demonstrated that mAbs against CD179a/b specifically detect B-LBL tissues. Although an examination of a larger number of lymphoma tissues is required to confirm their reliability, the application of these mAbs in the immunohistochemical examination of lymphoma tissues should contribute to a precise diagnosis of B-lineage lymphomas.

## Acknowledgements

This work was supported in part by Health and Labour Sciences Research Grants from the Ministry of Health, Labour and Welfare of Japan and MEXT, KAKENHI 15019129, JSPS, KAKENHI 15390133 and 15590361. This work was also supported by a grant from the Japan Health Sciences Foundation for Research on Health Sciences Focusing on Drug-Innovation. Additional support was provided by a grant from Sankyo Foundation of Life Science.

We thank M Sone and S Yamauchi for their excellent secretarial works. We also thank Dr S Hakomori (Washington University) and Otsuka Assay Laboratories for gifting CD77 mAb 1A4.

## References

1 Sakaguchi N, Melchers F. λ5, a new light-chain-related locus selectively expressed in pre-B lymphocytes. Nature 1986;324:579–582.
2 Kudo A, Melchers F. A second gene, VpreB in the λ5 locus of the mouse, which appears to be selectively expressed in pre-B lymphocytes. EMBO J 1987;6: 2267–2272.
3 Bauer SR, Kudo A, Melchers F. Structure and pre-B lymphocyte restricted expression of the VpreB in humans and conservation of its structure in other mammalian species. EMBO J 1988;7:111–116.
4 Hollis GF, Evans RJ, Stafford-Hollis JM, *et al.* Immunoglobulin λ light-chain-related genes 14.1 and 16.1 are expressed in pre-B cells and may encode the human immunoglobulin ω light-chain protein. Proc Natl Acad Sci USA 1989;86:5552–5556.
5 Schiff C, Bensmanna M, Gulglielmi P, *et al.* The immunoglobulin λ-like gene cluster (14.1, 16.1 and Fl1) contains gene(s) selectively expressed in pre-B cells and is the human counterpart of the mouse λ5 gene. Int Immunol 1990;2:201–207.
6 Karasuyama H, Kudo A, Melchers F. The proteins encoded by the VpreB and λ5 pre-B cell specific genes can associate with each other and with μ heavy chain. J Exp Med 1990;172:969–972.
7 Tsubata T, Reth M. The products of pre-B cell-specific genes (λ5 and VpreB) and the immunoglobulin μ chain form a complex that is transported onto the cell surface. J Exp Med 1990;172:973–976.
8 Karasuyama H, Rolink A, Shinkai Y, *et al.* The expression of VpreB/λ5 surrogate light chain in early bone marrow precursor B cells of normal and B cell-deficient mutant mice. Cell 1994;77:133–143.
9 Lassoued K, Nunez CA, Billips L, *et al.* Expression of surrogate light chain receptors is restricted to a late stage in pre-B cell differentiation. Cell 1993;73:73–86.
10 Tsuganezawa K, Kiyokawa N, Matsuo M, *et al.* Flow cytometric diagnosis of the cell lineage and developmental stage of acute lymphoblastic leukemia by novel monoclonal antibodies specific to human preB cell receptor. Blood 1998;92:4317–4324.
11 Brunning RD, Borowitz M, Matutes E, *et al.* Precursor B lymphoblastic leukaemia/lymphoblastic lymphoma (precursor B-cell acute lymphoblastic leukaemia). In: Jaffe ES, Harris NL, Stein H, Vardiman JW (eds). Pathology & Genetics: Tumours of Haematopoietic and Lymphoid Tissues. IARC Press: Lyon, 2001, pp 111–114.
12 Gatter K, Delsol G. B-cell lymphoblastic lymphoma. In: Gatter K, Delsol G (eds). The Diagnosis of Lymphoproliferative Diseases. Oxford University Press: Oxford, 2002, pp 59–63.
13 Ishii Y, Takami T, Yuasa H, *et al.* Two distinct antigen systems in human B lymphocytes: identification of cell surface and intracellular antigens using monoclonal antibody. Clin Exp Immunol 1984;58:183–192.
14 Ishii Y, Kon S, Takei T, *et al.* Four distinct antigen systems on human thymus and T cells defined by monoclonal antibodies: immunohistological and immunochemical studies. Clin Exp Immunol 1983;53: 31–40.
15 Fujimoto J, Ishimoto K, Kiyokawa N, *et al.* Immunocytological and immunochemical analysis on the common acute lymphoblastic leukemia antigen (CALLA): evidence that CALLA on ALL cells and granulocytes are structurally related. Hybridoma 1988;7:227–236.
16 Ishii E, Fujimoto J, Tanaka S, *et al.* Immunohistochemical analysis on normal nephorogenesis and Wilms' tumor using monoclonal antibodies reactive with lymphohaematopoietic antigens. Virchows Arch A Pathol Anat Histopathol 1987;411:315–322.
17 Neth O, Seidemann K, Jansen P, *et al.* Precursor B-cell lymphoblastic lymphoma in childhood and adolescence: clinical features, treatment, and results in trials NHL-BFM 86 and 90. Med Pediatr Oncol 2000;35: 20–27.
18 Kavan P, Kabickova E, Gajdos P, *et al.* Treatment of children and adolescents with non-Hodgkin's lymphoma (results based on the NHL Berlin–Frankfurt–Munster 90 protocols). Cas Lek Cesk 1999;138:40–46.
19 Kung PC, Long JC, McCaffrey RP, *et al.* Terminal deoxynucleotidyl transferase in the diagnosis of leukemia and malignant lymphoma. Am J Pathol 1978;64:788–794.
20 Mertelsmann R, Moore MA, Clarkson B. Methods and clinical relevance of terminal deoxynucleotidyl transferase determination in leukemic cells. Haematol Blood Transfus 1981;26:68–72.
21 Orazi A, Cattoretti G, Jphn K, *et al.* Terminal deoxynucleotidyl transferase staining of malignant lymphomas in paraffin sections. Mod Pathol 1994;7: 582–586.
22 Kaleem Z, Crawford E, Pathan MH, *et al.* Flow cytometric analysis of acute leukemias. Diagnostic utility and critical analysis of data. Arch Pathol Lab Med 2003;127:42–48.
23 Hsiao CH, Su IJ. Primary cutaneous pre-B lymphoblastic lymphoma immunohistologically mimics Ewing sarcoma/primitive neuroectodermal tumor. J Formos Med Assoc 2003;102:193–197.

# Induction of Apoptosis in Human Myeloid Leukemic Cells by 1′-Acetoxychavicol Acetate through a Mitochondrial- and Fas-Mediated Dual Mechanism

**Keisuke Ito,[1] Tomonori Nakazato,[1] Akira Murakami,[3] Kenji Yamato,[4] Yoshitaka Miyakawa,[1] Taketo Yamada,[2] Nobumichi Hozumi,[5] Hajime Ohigashi,[3] Yasuo Ikeda,[1] and Masahiro Kizaki[1]**

Departments of [1]Internal Medicine and [2]Pathology, Division of Hematology, Keio University School of Medicine, Tokyo, Japan; [3]Division of Food Science Biotechnology, Graduate School of Agriculture, Kyoto University, Kyoto, Japan; [4]Molecular Cellular Oncology and Microbiology, Graduate School, Tokyo Medical and Dental University, Tokyo, Japan; and [5]Institute of Biological Science, Science University of Tokyo, Chiba, Japan

## ABSTRACT

*Purpose:* **The purpose of this investigation was to determine the antileukemic effects of 1′-acetoxychavicol acetate (ACA) obtained from rhizomes of the commonly used ethno-medicinal plant *Languas galanga* (Zingiberaceae).**

*Experimental Design:* **We evaluated the effects of ACA on various myeloid leukemic cells *in vitro* and *in vivo*. We further examined the molecular mechanisms of ACA-induced apoptosis in myeloid leukemic cells.**

*Results:* **Low-dose ACA dramatically inhibited cellular growth of leukemic cells by inducing apoptosis. Because NB4 promyelocytic leukemic cells were most sensitive to ACA, we used NB4 cells for further analyses. Production of reactive oxygen species triggered ACA-induced apoptosis. ACA-induced apoptosis in NB4 cells was in association with the loss of mitochondrial transmembrane potential ($\Delta\Psi m$) and activation of caspase-9, suggesting that ACA-induced death signaling is mediated through a mitochondrial oxygen stress pathway. In addition, ACA activated Fas-mediated apoptosis by inducing of casapse-8 activity. Pretreatment with the thiol antioxidant *N*-acetyl-L-cysteine (NAC) did not inhibit caspase-8 activation, and the antagonistic anti-Fas antibody ZB4 did not block generation of reactive oxygen species, indicating that both pathways were involved independently in ACA-induced apoptosis. Furthermore, ACA had a survival advantage *in vivo* in a nonobese diabetic/severe combined immunodeficient mice leukemia model without any toxic effects.**

*Conclusions:* **We conclude that ACA induces apoptosis in myeloid leukemic cells via independent dual pathways. In addition, ACA has potential as a novel therapeutic agent for the treatment of myeloid leukemia.**

## INTRODUCTION

1′-Acetoxychavicol acetate (ACA) is present in seeds and rhizomes of *Languas galanga* (Zingiberaceae), which is used as a traditional condiment in Thailand and other countries in Southeast Asia (1). Recently, it has been reported that ACA inhibits chemically induced tumor formation and potently suppresses cellular growth of Ehrlich ascites tumor cells (2, 3). Other studies have demonstrated that this compound suppresses tumor promoter-induced EBV activation *in vitro* (1); ACA has subsequently been shown to inhibit skin tumor promotion in mice and both colonic aberrant crypt foci and adenocarcinoma formation in rats (4–7). ACA is also known to reduce superoxide anion production by inhibiting the xanthine oxidase and NADPH oxidase systems (7, 8), and this activity has been suggested to be partly responsible for its cancer chemopreventive effects (9). However, the mechanism of ACA-induced apoptosis remains unclear, and the effects of ACA on human leukemic cells have never been investigated.

Caspases are believed to play a crucial role in mediating various apoptotic responses. A model has been proposed in which two different caspases, caspase-8 and -9, mediated distinct types of apoptotic stimuli (10, 11). The cascade led by caspase-8 is involved in death receptor-mediated apoptosis such as the one triggered by Fas (also known as APO-1 or CD95). The death receptor, Fas, contains an intracytoplasmic death domain that mediates interactions with the adapter molecule Fas-associated death domain (FADD). FADD associates, in turn, with procaspase-8. Ligation of Fas by Fas ligand results in sequential recruitment of FADD and procaspase-8 to the death domain of Fas to form the death-inducing signaling complex, leading to cleavage of procaspase-8, with the consequent generation of active caspase-8. Caspase-8 then activates downstream effector caspases through cleavage of Bid, committing the cell to apoptosis (12). The mechanisms by which antineoplastic cytotoxic drugs kill leukemic cells are not well understood, although the activation of caspase-3 has been involved in the important signaling pathway of apoptosis (13). Recent observations have resulted in the suggestion that interactions between Fas and Fas ligand may mediate cytotoxic killing of at least some leukemic cell lines (14). On the other hand, the caspase pathway headed by caspase-9 is thought to mediate cytotoxic drug-induced apoptosis. Cytotoxic drugs induce generation of reactive oxygen species (ROS), leading to loss of

Received 8/1/03; revised 11/24/03; accepted 12/13/03.
**Grant support:** Grants from the Ministry of Education, Culture, Sports, Science, and Technology of Japan.
The costs of publication of this article were defrayed in part by the payment of page charges. This article must therefore be hereby marked *advertisement* in accordance with 18 U.S.C. Section 1734 solely to indicate this fact.
**Requests for reprints:** Masahiro Kizaki, Department of Internal Medicine, Division of Hematology, Keio University School of Medicine, 35 Shinanomachi, Shinjuku-ku, Tokyo 160-8582, Japan. Phone: 81-3-5363-3785; Fax: 81-3-3353-3515; E-mail: makizaki@sc.itc.keio.ac.jp.

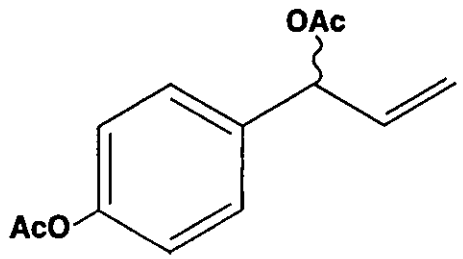


*Fig. 1* Chemical structure of (1′*R*,*S*′)-1′-acetoxychavicol acetate.

mitochondrial transmembrane potential ($\Delta\Psi m$) and the release of apoptogenic proteins such as cytochrome *c* and Smac/DIABLO from the mitochondria into the cytosol. The subsequent interaction of cytochrome *c* with Apaf-1 protein results in the recruitment of procaspase-9. Activation of procaspase-9 within this multiprotein complex, the apoptosome, results in the processing of caspase-3 and subsequently contributes to apoptotic cell death (15–17). The link between caspase-8 and caspase-9 is provided by caspase-8 cleavage of the proapototic Bid protein, whose truncated form is inserted into the mitochondrial outer membrane and promotes cytochrome *c* release and consequent activation of the apoptosome (18, 19). Anticancer drug-induced apoptosis was generally mediated through either a caspase-8 or caspase-9 pathway.

In the present study, we showed for the first time that a natural product, ACA, dramatically inhibits viability of myeloid leukemic cells via the induction of apoptosis through two different pathways. We further investigated the molecular mechanisms of ACA-induced cell cycle arrest and apoptosis in myeloid leukemic cells *in vitro*, as well as survival advantage with ACA *in vivo*.

## MATERIALS AND METHODS

**Cell Cultures.** The NB4 promyelocytic leukemia cell line was a gift of Dr. M. Lanotte (Hôpital St. Louis, Paris, France; Ref. 20), and the retinoic acid-resistant acute promyelocytic leukemia cell line UF-1 was established in our laboratory from a relapsed patient with acute promyelocytic leukemia who was treated with all-*trans*-retinoic acid (21). The human leukemic cell lines including HL-60 and K562 were obtained from the Japan Cancer Research Resources Bank (Tokyo, Japan). Bone marrow samples from patients with acute myeloid leukemia (AML) and mononuclear cells from a healthy donor were obtained according to appropriate Human Protection Committee validation at Keio University School of Medicine (Tokyo, Japan) and with written informed consent. Morphology was evaluated from cytospin slide preparations with Giemsa staining, and viability was assessed by trypan blue dye exclusion. Cells were maintained in RPMI 1640 (Life Technologies, Inc., Grand Island, NY) with 10% fetal bovine serum (Life Technologies, Inc.), 100 units/ml penicillin, and 100 μg/ml streptomycin in a humidified atmosphere with 5% $CO_2$. UF-1 cells were grown in RPMI 1640 with 15% fetal bovine serum (Hyclone Laboratories, Logan, UT) under standard culture conditions.

**Reagents.** ACA was synthesized as described previously (1) and dissolved in DMSO at a stock concentration of 20 mM. Synthetic (1′*R*,*S*′)-ACA (Fig. 1) has an identical suppressive activity to natural (1′*S*)-ACA as evaluated by tumor promoter-induced EBV activity (22). The pan-caspase inhibitor Z-VAD-FMK (Calbiochem, La Jolla, CA) and caspase-8 and -9 inhibitors [Z-IETD-FMK and LEHD-CHO, respectively (MBL, Nagoya, Japan)] were dissolved in DMSO (Sigma, St. Louis, MO) at a stock concentration of 100 mM, stored at −20°C, and protected from light. The final DMSO concentrations in the medium were not greater than 0.1%. *N*-acetyl-L-cysteine (NAC) and buthionine sulfoximine were purchased from Sigma.

**Cell Cycle Analysis.** Cells ($1 \times 10^6$) were suspended in hypotonic solution [0.1% Triton X-100, 1 mM Tris-HCl (pH 8.0), 3.4 mM sodium citrate, and 0.1 mM EDTA] and stained with 50 μg/ml propidium iodide. DNA content was analyzed by FACSCalibur (Becton Dickinson, San Jose, CA). The population of cells in each cell cycle phase was determined using Cell ModiFIT software (Becton Dickinson).

**Assays for Apoptosis.** Apoptosis was determined based on morphological change. Apoptotic cells were quantified by annexin V-FITC and propidium iodide double staining using a staining kit purchased from PharMingen (San Diego, CA). Induction of apoptosis was also detected by DNA fragmentation assay. The $\Delta\Psi m$ was determined by flow cytometry using rhodamine 123 (Sigma). Briefly, cells were washed twice with PBS and incubated with 1 μg/ml rhodamine 123 at 37°C for 30 min. Rhodamine 123 intensity was determined by flow cytometry.

**Caspase Assays.** Caspase-related protease activity was determined by using a commercially available kit (PharMingen) according to the manufacturer's instructions. Briefly, cells were fixed and permeabilized using the Cytofix/Cytoperm for 20 min at 4°C, pelleted, and washed with Perm/Wash buffer (PharMingen). Cells ($1 \times 10^6$) were then stained with polyclonal antibody against the active form of caspase-3, -9, and -8 (0.25 mg/liter; PharMingen) for 20 min at room temperature; washed in Perm/Wash buffer; stained with goat antirabbit FITC (Super Techs, Bethesda, MD); and analyzed via flow cytometry. For caspase inhibitor assay, cells were pretreated with a synthetic pan-caspase inhibitor (20 μM Z-VAD-FMK) and caspase-8 and -9 inhibitors (50 μM Z-IETD-FMK and LEHD-CHO, respectively) for 1 h before the addition of ACA.

**Measurement of ROS Production.** To assess the generation of ROS, control and ACA-treated cells were incubated with 5 μM dehydroxy ethidium (Molecular Probes, Eugene, OR), which is rapidly oxidized to a fluorescent intercalator, ethidium, by cellular oxidants. Cells ($1 \times 10^5$) were stained with 5 μM dehydroxy ethidium for 15 min at 37°C and then washed and resuspended in PBS. The oxidative conversion of dehydroxy ethidium to ethidium was analyzed by flow cytometry. To measure intracellular glutathione (GSH) levels, cells ($1 \times 10^5$) were stained with 20 μM 5-chloromethyl fluorescein diacetate (Molecular Probes) for 30 min at 37°C and then analyzed by flow cytometry.

**Cell Lysate Preparation and Western Blotting.** Cells were collected by centrifugation at $700 \times g$ for 10 min, and then the pellets were resuspended in lysis buffer [1% NP40, 1 mM phenylmethylsulfonyl fluoride, 40 mM Tris-HCl (pH 8.0), and 150 mM NaCl] at 4°C for 15 min. Mitochondrial and cytosolic fractions were prepared with digitonin-nagarse treatment. Protein concentrations were determined using a DC protein assay system (Bio-Rad, Richmond, CA). Cell lysates (15 μg protein/

lane) were fractionated in 12.5% or 7.5% SDS-polyacrylamide gels before being transferred to Immobilon-P membrane (Millipore, Bedford, MA) according to a standard protocol. Antibody binding was detected by using the enhanced chemiluminescence kit with hyper-enhanced chemiluminescence film (Amersham, Buckinghamshire, United Kingdom). β-Actin was used as an indicator for equality of lane loading. The following antibodies were used in this study: anti-caspase-3, anti-caspase-8, anti-cytochrome *c*, and anti-Rb (PharMingen); anti-cyclin B (Cell Signaling Technology, Inc., Beverly, MA); anti-Fas and anti-Bid (MBL); and anti-Bcl-2, anti-BAX, anti-$p21^{CIP1/WAF1}$, anti-$p27^{KIP1}$, anti-poly(ADP-ribose) polymerase, and anti-β-actin (Santa Cruz Biotechnology, Santa Cruz, CA).

**Assays for Fas.** We analyzed the expression of Fas by incubating cells with monoclonal anti-Fas-FITC antibody (UB2; Immunotech, Nottingham, United Kingdom) or control mouse IgG1 FITC antibody for 30 min at 4°C and then analyzing them by flow cytometry. For Fas inhibitor assay, antagonistic ZB4 monoclonal antibody (MBL) was added at 250 ng/ml 1 h before treatment with 10 μM ACA or 200 ng/ml agonistic anti-Fas antibody (CH11; MBL).

**Immunoprecipitation.** After treatment with ACA, cells ($1.5 \times 10^6$) were washed twice in PBS and incubated with the cleavable cross-linker 3,3′-dithiobis[sulgosuccinimidyl-propionate] (Pierce Chemical Co., Rockford, IL) for 10 min at 4°C. The reaction was stopped by a 5-min incubation in PBS containing 10 mM ammonium acetate at 4°C. Cells were washed twice in PBS and lysed in lysis buffer for 15 min on ice. After centrifugation at 17,800 × *g* for 15 min, an antihuman FADD antibody (MBL) was added and reacted at 4°C overnight. Immune complexes were precipitated using protein A-Sepharose (Pharmacia Co., Orsay, France) and washed three times in lysis buffer. The precipitate was resuspended in Laemmli buffer containing 2.5% β-mercaptoethanol and boiled for 5 min. Samples were fractionated on 12.5% SDS-polyacrylamide gels before being transferred to Immobilon-P membranes (Millipore) according to a standard protocol. Caspase-8 content was analyzed by using antihuman caspase-8 antibody (PharMingen). To monitor loading of protein samples, the same membranes were reprobed with an anti-FADD antibody.

**Animal Model and Experimental Design.** We have established a human all-*trans*-retinoic acid-sensitive acute promy-

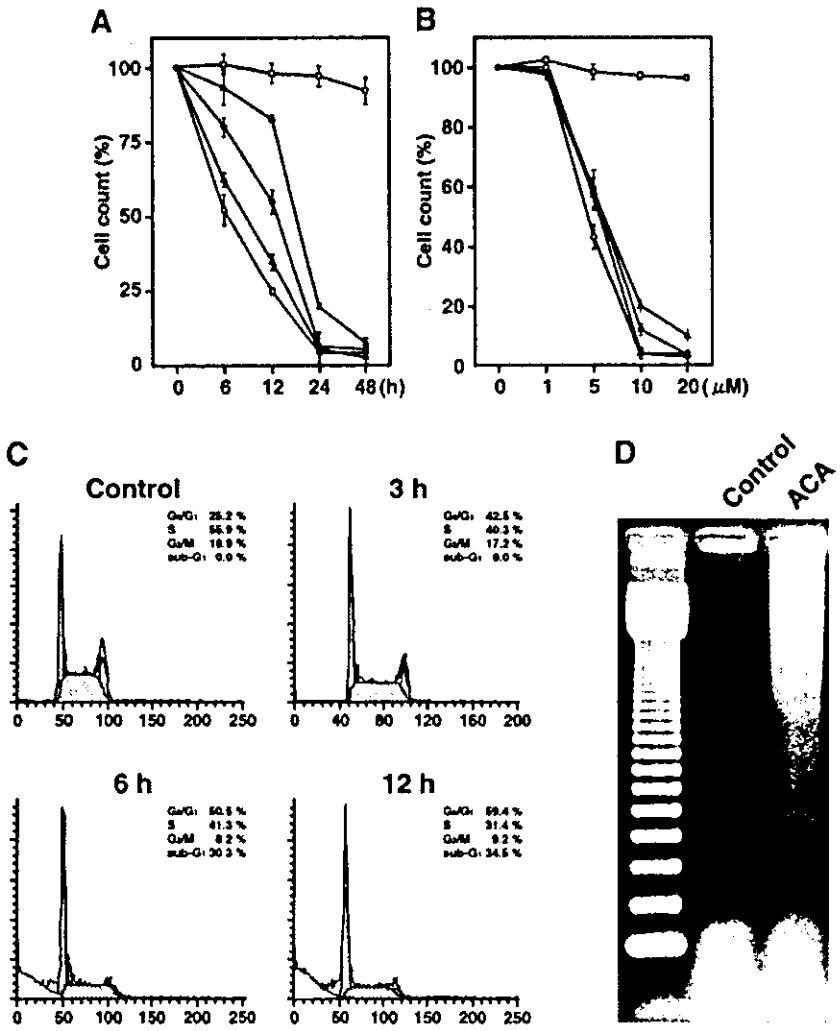


*Fig. 2* 1′-Acetoxychavicol acetate (ACA) inhibits cellular growth of myeloid leukemic cells via $G_0$-$G_1$ cell cycle arrest followed by apoptosis. *A* and *B*, various myeloid leukemic cells (NB4, ○; HL-60, △; UF-1, ▲; K562, ●) and bone marrow cells from a healthy donor (□) were treated with 10 μM ACA for various times (0–48 h) and at various concentrations (0–20 μM) for 24 h. Cell viability was assessed by trypan blue dye exclusion. Results are expressed as the mean of three duplicate experiments, and the SD was within 5% of the mean. *C*, cell cycle analysis. Cells were cultured with 10 μM ACA for the indicated time and then stained with propidium iodide as described in "Materials and Methods." DNA content was analyzed by means of flow cytometry. $G_0$-$G_1$, $G_2$-M, and S indicate the cell phase, and sub-$G_1$ DNA content refers to the portion of apoptotic cells. Each phase was calculated using the ModiFIT program. Three duplicate experiments were performed with similar results. *D*, agarose gel electrophoresis demonstrating DNA fragmentation in NB4 cells treated with 10 μM ACA for 4 h.

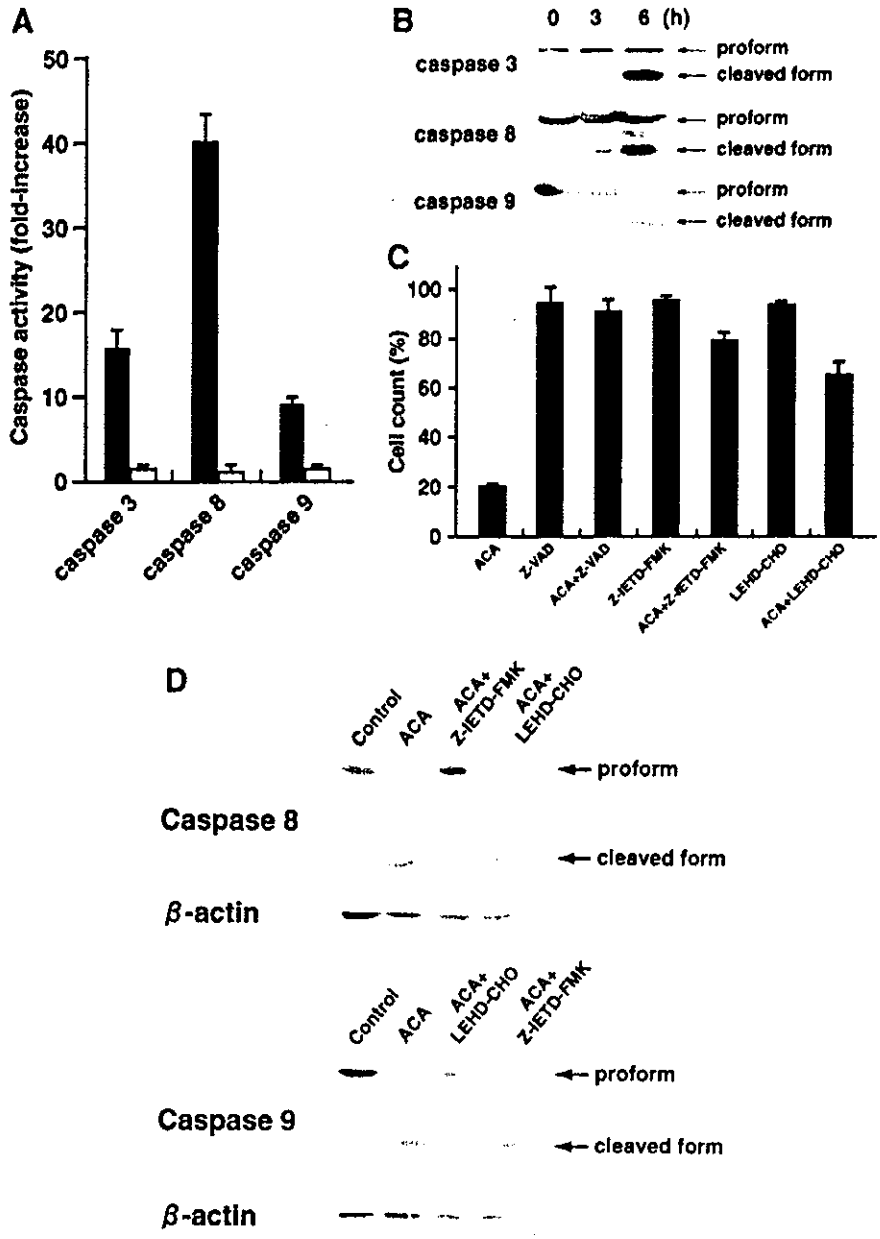


*Fig. 3* Effects of 1'-acetoxychavicol acetate (ACA) on caspase activation. *A*, cells were incubated with 10 μM ACA for 3 h and analyzed for activities of various caspases by fluorescence-activated cell-sorting analysis and colorimetric assay. ACA treatment (■) significantly increased caspase-3, -8, and -9 activities. Combination of ACA and each caspase inhibitor (□) blocked caspase activities. *B*, time course of caspase-3, -8, and -9 cleavage in ACA-treated NB4 cells. Cells were cultured with 10 μM ACA for the indicated times and analyzed by immunoblotting with anti-caspase-3, -8, and -9 antibodies. *C*, effects of caspase inhibitors on ACA-treated NB4 cells. Inhibition of ACA-induced apoptosis of NB4 cells was estimated in a coculture with a series of caspase inhibitors. Cells were preincubated with each caspase inhibitor [20 μM Z-VAD-FMK (pan-caspase inhibitor), 50 μM Z-IETD-FMK (caspase-8 inhibitor), and 50 μM LEHD-CHO (caspase-9 inhibitor)] for 1 h before the addition of 10 μM ACA. For *A* and *C*, values represent the mean ± SD for three separate experiments performed in triplicate. *D*, effects of caspase inhibitors on ACA-induced caspase cleavage. Cells were preincubated with 50 μM Z-IETD-FMK and 50 μM LEHD-CHO for 1 h and then cultured with10 μM ACA for 6 h. Protein lysates were separated with 10% SDS-PAGE and analyzed by blotting with anti-caspase-8 and -9 or β-actin antibodies.

elocytic leukemia model in a nonobese diabetic (NOD)/severe combined immunodeficient mice system using NB4 cells (23). Briefly, NOD/severe combined immunodeficient mice (The Jackson Laboratory, Bar Harbor, ME) were pretreated with 3 Gy of total body irradiation, which is a sublethal dose that was expected to enhance the acceptance of xenografts. Subsequently, NB4 cells ($1 \times 10^7$) in their logarithmic growth phase were inoculated s.c. into NOD/severe combined immunodeficient mice. Inoculated NB4 cells formed s.c. tumors at the injection site, and cells grew rapidly. Fourteen days after implantation of the cells, mice with the transplanted cells were randomly assigned to be injected with PBS ($n$ = 15) or 3 mg/kg ACA ($n$ = 15) via i.p. injection for 3 days. The study was approved by the Animal Care and Use Committee at the Keio University School of Medicine. Mice were routinely monitored to determine their general condition, and survival times were used to determine therapeutic efficacy. When the mice showed severe wasting, or when observations were finished, mice were sacrificed according to the United Kingdom Coordinating Committee on Cancer Research guidelines, and the day of sacrifice was recorded (24).

## RESULTS

**Effects of ACA on Cellular Proliferation of Various Leukemia Cells.** We first investigated the effects of ACA on cellular proliferation in four myeloid leukemic cell lines [NB4, UF-1, HL-60, and K562]. ACA (10 μM) inhibited cellular

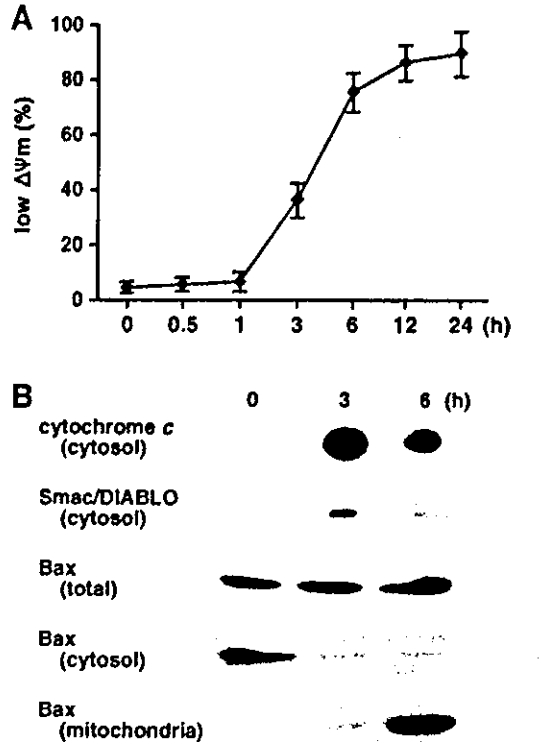


*Fig. 4* 1′-Acetoxychavicol acetate (ACA)-induced apoptosis is mediated through a mitochondrial pathway. *A*, NB4 cells were cultured with 10 μM ACA for 3 h, and rhodamine 123 fluorescence was analyzed by flow cytometry for the indicated times. *B*, expression of cytosolic cytochrome *c*, cytosolic Smac/DIABLO, total Bax, cytosolic Bax, and mitochondrial Bax in ACA-treated NB4 cells was assessed by Western blot analysis.

growth of all myeloid leukemic cells, but not normal bone marrow mononuclear cells from a healthy donor, in a dose- and a time-dependent manner (Fig. 2, *A* and *B*). Interestingly, ACA decreased cellular growth of NB4 cells with the lowest $IC_{50}$ (4.72 μM). Therefore, we used NB4 cells for subsequent investigations. Cultivation with ACA rapidly increased the population of cells in the $G_0$-$G_1$ phase with a reduction of cells in S phase, and a strong induction of apoptosis was shown by the appearance of a hypodiploid DNA peak with sub-$G_1$ DNA content 6 h after treatment (Fig. 2*C*). Apoptosis was assessed in terms of both morphological changes and DNA ladder formation. DNA fragmentation was confirmed by electrophoresis of genomic DNA extracted from NB4 cells treated with 10 μM ACA for 4 h (Fig. 2*D*). These results indicate that ACA led to cell cycle arrest at the $G_0$-$G_1$ phase followed by apoptosis.

**Effects of ACA on Caspase Activity.** Treatment with ACA for 3 h significantly induced caspase-3, -8, and -9 activities in NB4 cells (Fig. 3*A*). Various caspase inhibitors blocked caspase activities (Fig. 3*A*). We also found that ACA induced caspase-3, -8, and -9 activation as assessed by cleavage of proforms into the active cleaved forms using polyclonal antihuman casapase-3, -8, and -9 antibodies (Fig. 3*B*). Interestingly, ACA-induced caspase-8 activation was rapid, occurring within 3 h of treatment and before activation of caspase-3 and -9 (Fig. 3*B*). NB4 cells were treated with 10 μM ACA for 24 h, either alone or in combination with 20 μM Z-VAD-FMK (pan-caspase inhibitor), 50 μM Z-IETD-FMK (caspase-8 inhibitor), or 50 μM LEHD-CHO (caspase-9 inhibitor). Each caspase inhibitor alone did not have any effect on the proliferation of NB4 cells. ACA-induced apoptosis was almost completely blocked by treatment with Z-VAD-FMK, although Z-IETD-FMK and LEHD-CHO partially inhibited ACA-induced apoptosis in NB4 cells (Fig. 3*C*). Z-IETD-FMK and LEHD-CHO inhibited ACA-induced caspase-8 and -9 cleavage, respectively (Fig. 3*D*). These results suggest that ACA-induced apoptosis is associated with the activation of caspase-3, -9, and -8.

**ACA-Induced Death Signaling Is Mediated through the Mitochondrial Pathway.** After treatment with 10 μM ACA for 3 h, low rhodamine 123 staining in NB4 cells indicated an increase in the loss of $\Delta\Psi m$ in a time-dependent manner (Fig. 4*A*). ACA also induced a substantial release of cytochrome *c* and Smac/DIABLO from the mitochondria into the cytosol (Fig. 4*B*). In addition, ACA induced a translocation of Bax from the cytosol to the mitochondria within 3 h, whereas the protein accumulated in the mitochondria (Fig. 4*B*). These results suggest that the mitochondrial-dependent pathway plays an important role in ACA-induced apoptosis.

**Expression of Cell Cycle- and Apoptosis-Associated Proteins in ACA-Treated NB4 Cells.** To characterize the molecular mechanism of ACA-induced cell cycle arrest followed by apoptosis in NB4 cells, we examined the expression of cell cycle- and apoptosis-associated proteins during treatment with

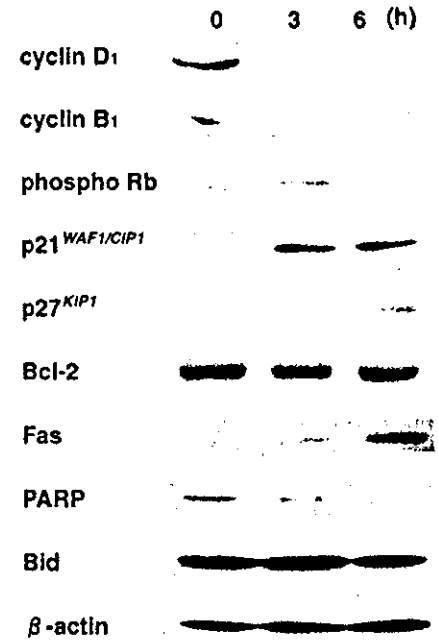


*Fig. 5* Expression of the apoptosis- and cell cycle-associated proteins. NB4 cells were treated with 10 μM 1′-acetoxychavicol acetate for the indicated time. Cell lysates (15 μg/lane) were fractionated on 12.5% SDS-polyacrylamide gels and analyzed by Western blotting with antibodies against apoptosis- and cell cycle-associated proteins [cyclin D1, cyclin B1, pSer-Rb, $p21^{WAF1/CIP1}$, $p27^{KIP1}$, Bcl-2, Fas, poly(ADP-ribose) polymerase, and Bid]. Reblotting with β-actin staining demonstrated that equal amounts of protein were present in each lane.

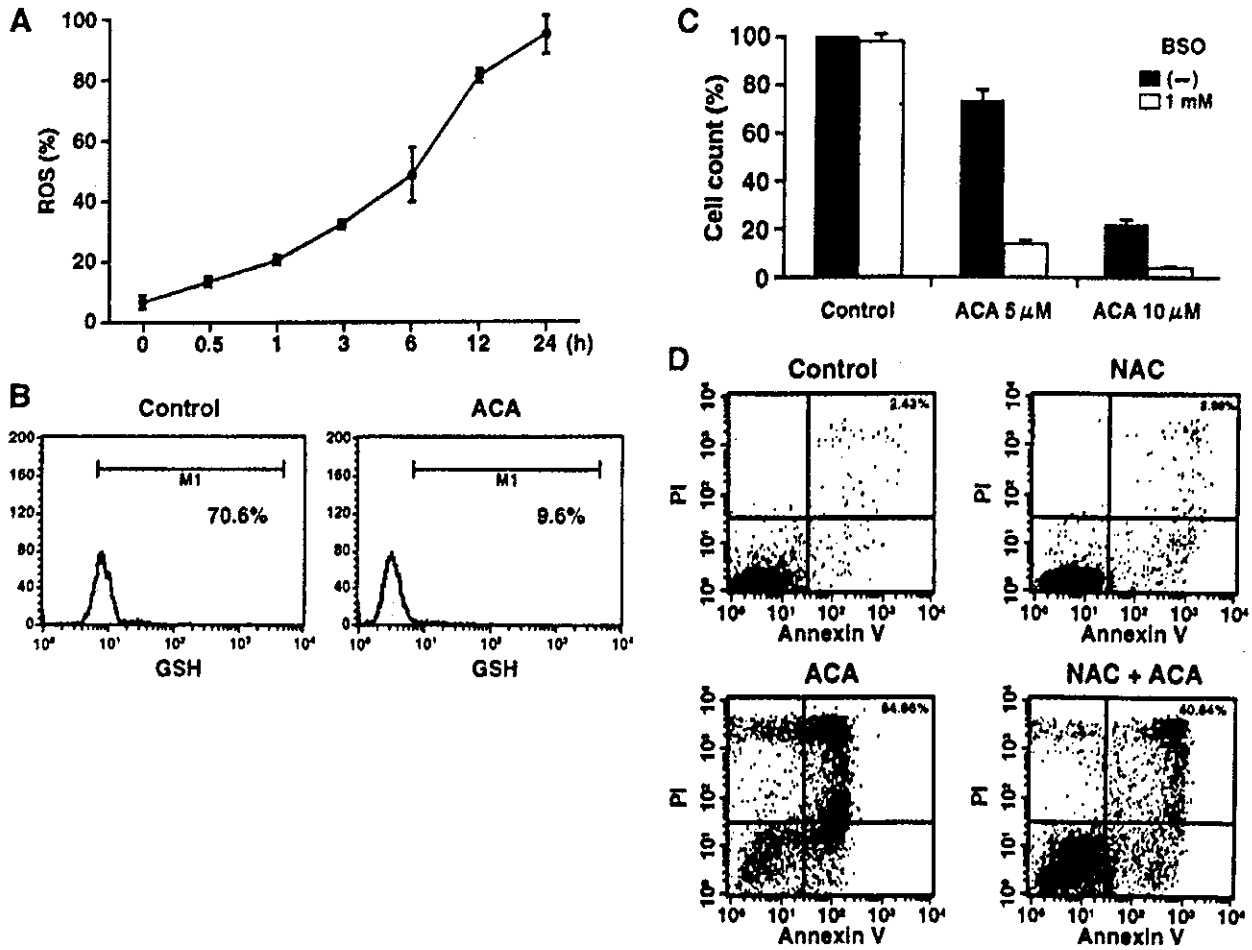


*Fig. 6* Effect of 1′-acetoxychavicol acetate (ACA) on generation of reactive oxygen species. *A*, NB4 cells were treated with 10 μM ACA for the indicated times, after which cells were labeled with an oxidative-sensitive dye (dehydroxy ethidium) and analyzed by flow cytometry to determine the percentage of cells displaying an increase in production of reactive oxygen species. *B*, generation of glutathione in ACA-treated NB4 cells. Cells were treated with 20 μM 5-chloromethyl fluorescein acetate for 30 min and then analyzed by flow cytometry. *C*, effects of buthionine sulfoximine on ACA-treated NB4 cells. Cells were treated with 5 or 10 μM ACA and then incubated without (■) or with (□) 1 mM buthionine sulfoximine for 12 h. Cell viability was assessed by trypan blue dye exclusion. *D*, cells were pretreated with 100 μM *N*-acetyl-L-cysteine and then treated with 10 μM ACA for 12 h, and induction of apoptosis was examined by annexin V/propidium iodide double staining.

ACA. Expression of $p21^{WAF1/CIP1}$, $p27^{KIP1}$, and Fas was increased in a time-dependent manner with dephosphorylation of Rb, reduction of cyclin D1 and B1 protein expression, and cleavage of poly(ADP-ribose) polymerase (Fig. 5). In contrast, ACA did not affect the expression of Bcl-2 or Bid protein (Fig. 5).

**Effects of ACA on Intracellular ROS Generation.** Within 0.5 h, NB4 cells treated with 10 μM ACA showed an increase in intracellular ROS compared with control cells (Fig. 6*A*), corresponding to the reduction of intracellular GSH (Fig. 6*B*); 1 mM buthionine sulfoximine, a specific inhibitor of γ-glutamylcysteine synthetase, induced GSH depletion and synergically enhanced ACA-induced apoptosis (Fig. 6*C*). Treatment with a thiol antioxidant, NAC, an excellent supplier of GSH, attenuated but did not completely inhibit ACA-induced apoptosis with complete inhibition of ROS generation in NB4 cells (Fig. 6*D*). These results indicate that ROS generation plays a partial role in ACA-induced apoptosis, but another pathway may also contribute to the ACA-induced apoptotic pathway in NB4 cells.

**ACA Activates Fas/Fas Ligand-Mediated Apoptosis in NB4 Cells.** ACA rapidly activated caspase-8 and -9, and each specific inhibitor partially blocked ACA-induced apoptosis in NB4 cells, respectively (Fig. 3*B*). For that reason, we investigated whether the Fas-mediated pathway was involved in ACA-induced apoptosis. Suppression of Fas by 12-h exposure to antagonistic anti-Fas antibody ZB4 dramatically inhibited ACA-induced apoptosis, similar to that of agonistic anti-Fas antibody (CH11) in NB4 cells (Fig. 7, *A* and *B*). However, longer exposure (24 h) to ZB4 partially blocked ACA-induced cell proliferation (Fig. 7*A*). CH11-induced apoptosis in NB4 cells was completely blocked by ZB4 (Fig. 7, *A* and *B*). Corresponding to these results, expression of Fas on the plasma membrane was significantly increased immediately after ACA treatment (Fig. 7*C*) with induction of Fas ligand (data not shown). The death-inducing signaling complex was also formed in NB4 cells treated with ACA (Fig. 7*D*). These results indicate that the apoptotic

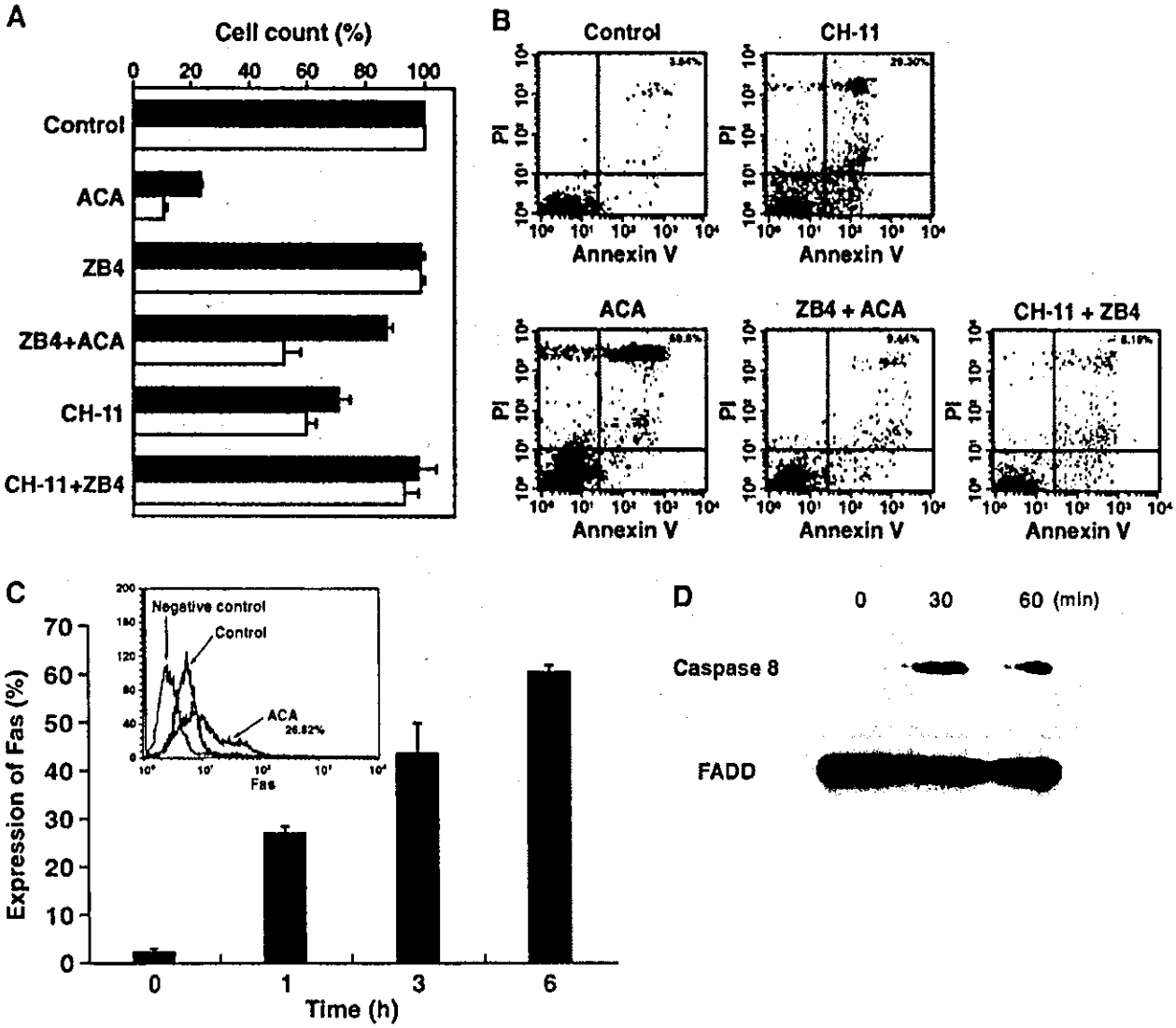


*Fig. 7* 1'-Acetoxychavicol acetate (ACA)-induced apoptosis via the Fas pathway. *A*, antagonistic anti-Fas antibody blocks ACA-induced apoptosis in NB4 cells. NB4 cells were preincubated for 1 h in the presence of 500 ng/ml ZB4 antagonistic anti-Fas-antibody for 12 (■) or 24 h (□) and then treated with 10 μM ACA and 250 ng/ml Fas-IgG (CH11), after which cell viability was assessed by trypan blue dye exclusion. Results are expressed as the means ± SD of three duplicate experiments. *B*, induction of apoptosis was examined by annexin V/propidium iodide double staining. These data represent three separate experiments. *C*, flow cytometric analysis of Fas expression on the plasma membrane of tumor cells. NB4 cells were treated with 10 μM ACA for 1 h, and Fas expression was determined by flow cytometry using anti-Fas IgG FITC antibody (UB2). We used antimouse IgG1 and IgG2a FITC antibody as the negative control. Results are representative of three duplicate experiments. A representative case is shown in the *inset*. *D*, ACA-induced death-inducing signaling complex formation. NB4 cells were stimulated with 10 μM ACA for the indicated times. Proteins were extracted and immunoprecipitated with an antibody directed against Fas-associated death domain. After blotting to nitrocellulose membranes, Western blot analysis was performed using an antibody directed against caspase-8.

pathway related to Fas/Fas ligand also seems to be involved in ACA-induced apoptosis.

**ACA-Induced Apoptosis in NB4 Cells Mediated through Dual Pathways.** Because Bid protein, which is known to link caspases-8 and -9, was not cleaved during treatment with ACA (Fig. 5), we hypothesized that Fas/Fas ligand- and ROS-dependent pathways are independently activated during ACA-induced cell death. We thus investigated the effects of antagonistic anti-Fas antibody ZB4 on ROS generation and the effects of NAC on the enzymatic activity of caspase-8. Inhibition of the Fas pathway by ZB4 did not affect ROS generation, and the activity of caspase 8 was not altered during NAC treatment (Fig. 8, *A* and *B*). In addition, costimulation of ZB4 and NAC additively inhibited ACA-induced apoptosis (Fig. 8*C*), indicating that ROS generation was completely independent of the Fas/Fas ligand-mediated pathway.

**Effects of ACA on Primary Samples from Patients with AML.** We examined the effects of ACA on primary AML cells from 10 patients (Table 1). Representative cases of ACA-induced apoptosis and generation of ROS are shown in Fig. 9, *A*

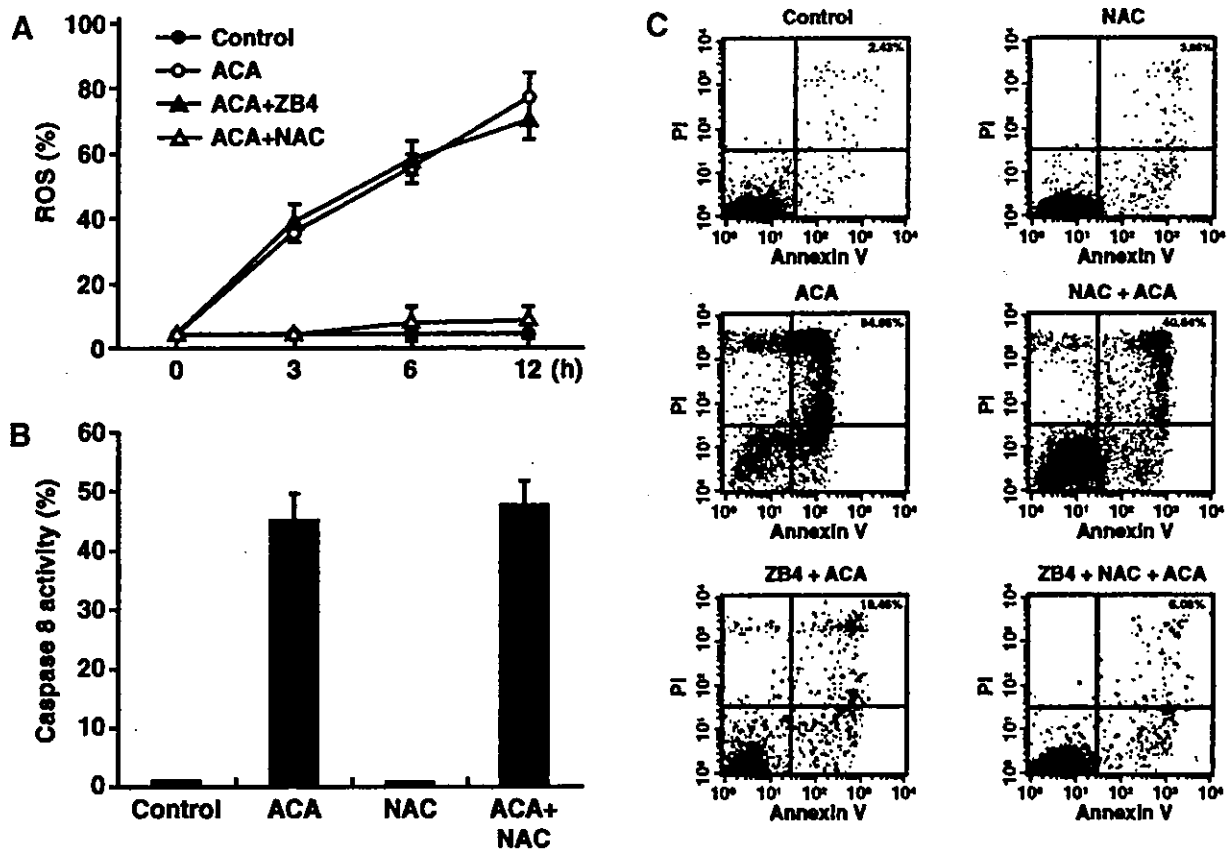


*Fig. 8* *N*-Acetyl-L-cysteine (NAC) and ZB4 independently inhibited 1′-acetoxychavicol acetate (ACA)-induced apoptosis. *A*, generation of reactive oxygen species. NB4 cells were preincubated with 100 μM NAC or 500 ng/ml ZB4 for 1 h and then incubated with 10 μM ACA for the indicated times (0–12 h). After that, cells were labeled with dehydroxy ethidium and analyzed by flow cytometry to determine the percentage of cells displaying an increase in production of reactive oxygen species. *B*, casapase-8 activity. NB4 cells were preincubated with NAC and then incubated with 10 μM ACA for 12 h. Caspase-8 activity was measured by fluorescence-activated cell-sorting analysis and colorimetric assay. For *A* and *B*, values represent the mean ± SD for three separate experiments performed in triplicate. *C*, NB4 cells were pretreated with either 100 μM NAC, 500 ng/ml ZB4, or both agents for 1 h before ACA addition. Cells were then incubated with 10 μM ACA for 12 h. The percentage of apoptotic cells corresponds to the number of annexin V-positive cells.

and *B*. ACA remarkably inhibited cellular growth of freshly isolated cells from patients with AML by induction of apoptosis corresponding to induction of ROS generation (Fig. 9, *A* and *B*) and Fas and Fas ligand expression (data not shown). In contrast, ACA did not affect cellular growth of bone marrow mononuclear cells from healthy volunteers (Fig. 2, *A* and *B*). These results strongly supported the finding that induction of both Fas expression and ROS generation plays a crucial role in the effects of ACA on fresh myeloid leukemic cells, and ACA has potential as a treatment for patients with AML.

**Effects of ACA *in Vivo*.** Our *in vitro* data prompted us to examine whether the effects of ACA are equally valid *in vivo*. To evaluate the effect on survival, NB4-transplanted NOD/severe combined immunodeficient mice were treated with ACA (Fig. 10). The survival curves of mice in both groups are shown in Fig. 10, and the difference in survival between the two groups was statistically significant by log-rank test analysis ($P < 0.005$; Fig. 10). As shown in Fig. 10, ACA markedly improved overall survival. During the treatment, ACA-treated mice appeared healthy. In addition, pathological analysis at autopsy revealed no capsaicin-induced tissue changes in any of the organs (data not shown). These results suggest that ACA had no toxic effects on mice during this treatment.

## DISCUSSION

Natural products have been the mainstay of cancer chemotherapy for the past 30 years (25). For example, the main constituent of the plant *Catharanthus reseus* was the forerunner of the anticancer agents known as the *Vinca* alkaloids, vinblastine and vincristine. Both drugs were introduced to the clinical field in the late 1960s and have contributed to long-term remissions and cures of testicular teratoma, malignant lymphoma, lymphoblastic leukemia, and many other cancers. Natural products or their structural relatives now comprise about 50% of the drugs that are used for cancer chemotherapy. Therefore, it is an important project to discover novel anticancer agents from natural products through a routine examination of terrestrial plants and microorganisms. There have been a series of studies reporting that ACA, a natural product from edible plants in southeast-

*Table 1* Baseline characteristics of patients and effect of ACA[a] on primary AML cells[b]

| Patient no. | Age (yrs) | Sex | Diagnosis[c] | Blast[d] (%) | Annexin V-positive cells (%) | | | Fas-positive cells (%) | | |
|---|---|---|---|---|---|---|---|---|---|---|
| | | | | | Control | ACA | Fold-increase[e] | Control | ACA | Fold-increase[e] |
| 1 | 49 | M | AML (M1) | 87.0 | 12.4 | 94.2 | 7.6 | 10.3 | 56.9 | 5.5 |
| 2 | 30 | M | AML (M2) | 91.4 | 1.7 | 84.8 | 49.9 | 2.5 | 66.7 | 26.7 |
| 3 | 35 | F | AML (M4) | 86.8 | 7.8 | 89.4 | 11.5 | 5.4 | 45.3 | 8.4 |
| 4 | 58 | M | AML (M2) | 83.0 | 11.2 | 79.4 | 7.1 | 9.3 | 78.2 | 8.4 |
| 5 | 68 | F | AML (M1) | 81.6 | 19.5 | 84.7 | 4.4 | 10.5 | 53.2 | 5.1 |
| 6 | 56 | M | AML (M2) | 90.0 | 8.9 | 78.5 | 8.8 | 6.5 | 40.3 | 6.2 |
| 7 | 39 | M | AML (M3) | 93.0 | 9.4 | 87.1 | 9.3 | 7.3 | 78.9 | 10.8 |
| 8 | 27 | M | AML (M0) | 98.2 | 20.5 | 96.7 | 4.7 | 14.3 | 74.6 | 5.2 |
| 9 | 24 | F | AML (M3) | 81.0 | 4.1 | 78.5 | 19.1 | 9.5 | 64.3 | 6.8 |
| 10 | 49 | M | AML (M2) | 96.6 | 21.7 | 87.6 | 4.0 | 11.4 | 49.8 | 4.4 |

[a] ACA, 1'-acetoxychavicol acetate; AML, acute myeloid leukemia.
[b] Cells were separated by Lymphoprep sedimentation procedure and subsequently cultured with 10 μM ACA for 12 h.
[c] Diagnosis was based on French-American-British classification.
[d] Samples from patients were separated from bone marrow, and the percentage of blast cells are at diagnosis.
[e] Induction of apoptosis and Fas expression were expressed as fold increase of the percentage of control cells.

ern Asia, exhibits chemopreventive effects on various tumors (1–7). However, there have been no investigations regarding the effects of ACA on human leukemias. In this report, we propose for the first time that ACA induced apoptosis in myeloid leukemic cells mediated by dual pathways through mitochondrial oxidative stress and Fas/Fas ligand system.

We demonstrated that ACA suppressed the cellular growth of various myeloid leukemic cell lines and fresh samples via the induction of apoptosis. Mitochondria play an essential role in the death-signaling pathway. In general, permeability transition pore opening, collapse of the mitochondrial $\Delta\Psi m$ resulted in the rapid release of caspase activators such as cytochrome *c* into the cytoplasm (26). We demonstrated that the loss of $\Delta\Psi m$ increased within 3 h of treatment, a time frame parallel to that of induced apoptosis. Furthermore, caspase-3 was activated by ACA, and caspase-3 and caspase-9 inhibitors suppressed the apoptotic effects of ACA. Taken together, these results suggest that ACA-induced apoptosis in leukemic cells is associated with the loss of $\Delta\Psi m$ and with the activation of caspases, probably via the cytochrome *c*/Apaf-1/caspase-9 pathway. We further demonstrated that ACA had no influence on the expression of Bcl-2 or Bcl-$X_L$, but it up-regulated the levels of mitochondrial but not cytoplasmic Bax protein in NB4 cells in a time-dependent manner. Bax translocation to the mitochondria has been shown to reduce $\Delta\Psi m$, enhance cytochrome *c* release from the mitochondria, and activate caspases (27, 28).

We detected that ACA-induced apoptosis in myeloid leukemic cells was associated with an increase in the levels of intracellular ROS. It has been suggested that the generation of ROS is a common mechanism in one of the representative pathways of apoptosis through mitochondria by triggering cytochrome *c* release with the consequent Apaf-1-dependent activation of caspase-9 (26, 29). Oxidant and its compounds are capable of depleting GSH or damaging the cellular antioxidant defense system and can directly induce apoptosis (30–32). We demonstrated that ACA rapidly induced ROS generation and that pretreatment with antioxidant NAC inhibited ACA-induced apoptosis. In addition, buthionine sulfoximine, which reduces intracellular GSH contents, enhanced ACA-induced apoptosis. Recently, it has been reported that superoxide dismutases are target molecules of estrogen-induced apoptosis in leukemic cells identified by cDNA microarray assay and that inhibition of superoxide dismutase causes an accumulation of ROS and leads to the release of cytochrome *c* from the mitochondria (33). Most ACA-sensitive NB4 cells among the various leukemic cells used in this study were reported to have weak activities of antioxidant enzymes including glutathione peroxidase, catalase, and glutathione *S*-transferase (34, 35). These results suggest that ACA-induced apoptosis in leukemic cells is modulated by the cellular GSH redox system.

The role of membrane death receptor-mediated apoptosis is known to be one of the pathways to caspase-8 activation. On activation of death receptors by their ligation, the death receptors recruit the adapter molecule FADD by the death domain that is also present on FADD, followed by activation of caspase-8. We demonstrated that Fas ligand levels were increased in NB4 cells during treatment with ACA. NB4 cells were sensitive to Fas-induced apoptosis because agonistic anti-Fas antibody CH11 induced apoptosis, and antagonistic anti-Fas antibody ZB4 inhibited the induction of apoptosis in NB4 cells. In addition, ZB4 induced the expression of cell surface Fas in association with reduction in apoptotic cells. Moreover, we demonstrated that up-regulation of Fas ligand expression and formation of death-inducing signaling complex during treatment with ACA corresponded to activation of caspase-8. These results indicate that signaling by the Fas/Fas ligand system plays an important role in the apoptotic killing of NB4 cells by ACA.

The time-response curve of caspase-8 in ACA-treated NB4 cells was similar to that of caspase-9, suggesting that both proteases were active in this apoptotic pathway. Caspase-8 directly activates the downstream caspase, caspase-3. Caspase-9, which is activated by cytochrome *c* from mitochondria, can also activate caspase-3 (36, 37). In certain cells, the mitochondrial activation-mediated pathway has been shown to be required for Fas-mediated apoptosis (28). In these cells, Bid mediates the release of cytochrome *c* from mitochondria initiated by caspase-8 activation (18, 38). Therefore, Bid interconnects the extrinsic apoptotic pathway initiated by death receptors to the intrinsic

pathway of mitochondria-mediated apoptosis (39). In our study, the antioxidant NAC did not affect activation of caspase-8, and antagonistic anti-Fas antibody ZB4 did not inhibit ROS generation. Also, Bid protein was not cleaved by treatment of NB4 cells with ACA. ACA-induced apoptosis was reduced in an additive way when NB4 cells were pretreated with ACA or ZB4. From these results, we conclude that there are two different pathways (for mitochondrial oxidative stress-mediated and Fas-mediated cell death signaling) in ACA-treated NB4 cells.

Acute leukemia is a hematological neoplastic disorder and generally shows aggressive clinical manifestations with poor prognosis in the clinical setting. The therapeutic approach to acute leukemia is basically chemotherapy for achieving complete remission, but side effects and complications such as

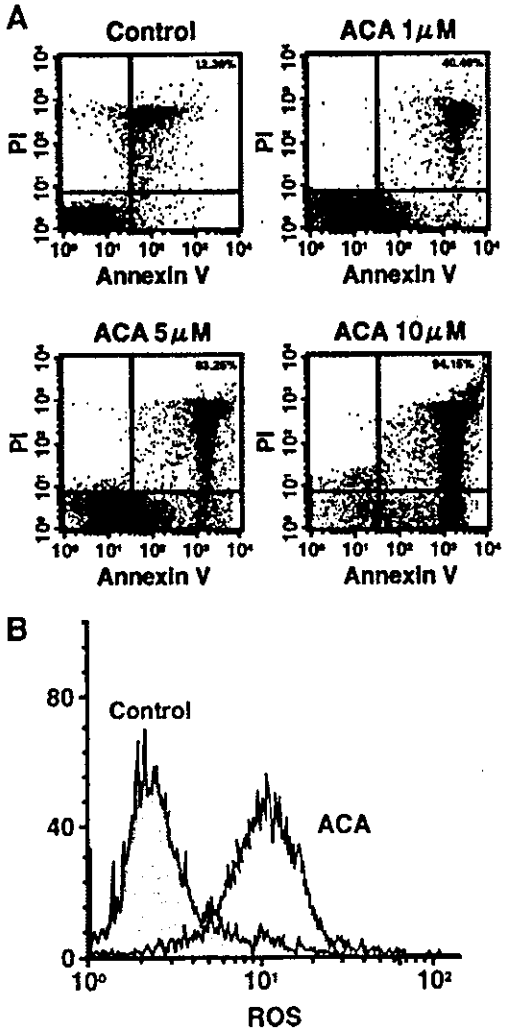


*Fig. 9* Effects of 1′-acetoxychavicol acetate on primary cells from patients with acute myeloid leukemia. Fresh leukemic cells from a patient were separated by the Lymphoprep sedimentation procedure and subsequently cultured with 10 μM 1′-acetoxychavicol acetate for 24 h. *A*, induction of apoptosis was measured by determining the number of annexin V-positive cells. *B*, generation of reactive oxygen species was measured by flow cytometry. Representative data from 10 patients with AML are shown.

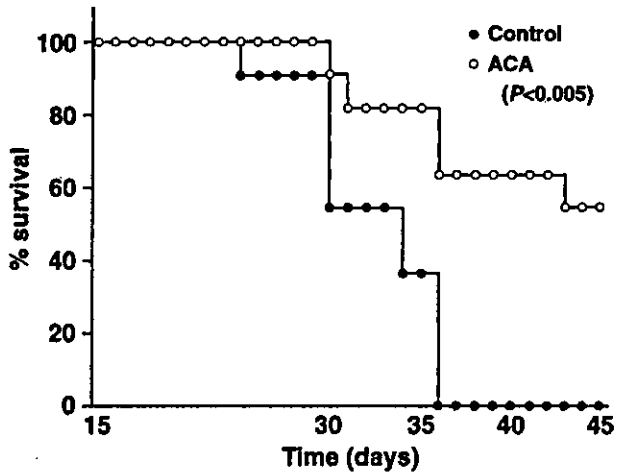


*Fig. 10* 1′-Acetoxychavicol acetate-mediated apoptosis of leukemic cells *in vivo* using a nonobese diabetic (NOD)/severe combined immunodeficient mice model. NB4 cells ($1 \times 10^7$) were inoculated s.c. into NOD/severe combined immunodeficient mice. Fourteen days after transplantation, PBS (control) or 1′-acetoxychavicol acetate (3 mg/kg) was given one time every 3 days. Kaplan-Meier survival curves between the experimental and control mice groups are statistically different by log-rank test ($P < 0.005$).

serious infection due to anticancer drugs are severe problems. In particular, side effects of anticancer drugs might be fatal in older patients or immunocompromised patients. In addition, repeated episodes of relapse of the disease may lead to refractory or chemotherapy-resistant leukemia. Therefore, novel effective therapeutic strategies are actively being sought in the world. A component of a traditional Thai condiment, ACA, is a natural compound, and it appears to be safer than current chemotherapeutic drugs. ACA remarkably inhibited cellular growth of primary cells from patients by the induction of apoptosis, whereas the same dose of ACA did not affect the cellular growth of bone marrow mononuclear cells from healthy volunteers, indicating that the effects of ACA are specific to neoplastic cells. In this study, we demonstrated the anticancer effects of ACA both *in vitro* and *in vivo*. Fas receptor is known to be constitutively expressed in the liver, indicating that the liver is very sensitive to Fas-induced apoptosis (40), and mice treated with an agonistic anti-Fas antibody died from hepatic failure caused by generalized apoptosis of hepatocytes (41). However, in our study, we could not observe any organ damage *in vivo*, suggesting that ACA had no toxic effects on mice during this treatment.

We conclude that ACA might be developed as a new, potent anticancer agent for the management of hematological malignancies. In addition, ACA has potential as a novel therapeutic agent to replace the more cytotoxic agents currently used to treat patients with myeloid leukemia.

## REFERENCES

1. Kondo A, Ohigashi H, Murakami A, Jiwajinda S, Koshimizu K. A potent inhibitor of tumor promoter-induced Epstein-Barr virus activation, 1′-acetoxychavicol acetate from Languas galangal, a traditional Thai condiment. Biosci Biotech Biochem 1993;57:1344–5.

2. Ohnishi M, Tanaka T, Makita H, et al. Chemopreventive effect of a xantine oxidase inhibitor, 1′-acetoxychavicol acetate, on rat oral carcinogenesis Jpn J Cancer Res 1996;87:349–56.

3. Moffat JJ, Hashimoto M, Kojima A, et al. Apoptosis induced by 1′-acetoxychavicol acetate in Ehrlich ascites tumor cells is associated with modulation of polyamine metabolism and caspase-3 activation. Carcinogenesis (Lond.) 2000;21:2151–7.

4. Nakamura A, Murakami Y, Ohto K, et al. Suppression of tumor promoter-induced oxidative stress and inflammatory responses in mouse skin by a superoxide generation inhibitor 1′-acetoxychavicol acetate. Cancer Res 1998;58:4832–9.

5. Murakami A, Ohura S, Nakamura Y, Koshimizu K, Ohigashi H. 1′-Acetoxychavicol acetate, a superoxide anion generation inhibitor, potently inhibits tumor promotion by 12-O-tetradecanoylphorbol-13-acetate in ICR mouse skin. Oncology (Basel) 1996;53:386–91.

6. Tanaka T, Makita H, Kawamori T, et al. A xantine oxidase inhibitor 1′-acetoxychavicol acetate inhibits azoxymethane-induced colonic aberrant crypt foci in rats. Carcinogenesis (Lond.) 1997;18:1113–8.

7. Tanaka T, Kawabata K, Kakumoto M, et al. Chemoprevention of azoxymethane-induced rat colon carcinogenesis by a xanthine oxidase inhibitor, 1′-acetoxychavicol acetate. Jpn J Cancer Res 1997;88:821–30.

8. Noro T, Sekiya T, Katoh M, et al. Inhibitor of xanthine oxidase from Alpinia galanga. Chem Pharm Bull 1998;36:244–8.

9. Pence CB, Reiners JJ Jr. Murine epidermal xanthine oxidase activity: correlation with degree of hyperplasia induced by tumor promoters. Cancer Res 1987;47:6388–92.

10. Sun XM, MacFarlane M, Zhuang J, et al. Distinct caspase cascades are initiated in receptor-mediated and chemical-induced apoptosis. J Biol Chem 1999;274:5053–60.

11. Zhuang J, Cohen GM. Release of mitochondrial cytochrome c is upstream of caspase activation in chemical-induced apoptosis in human monocytic tumor cells. Toxicol Lett 1998;102:121–9.

12. Ashkenazi A, Dixit VM. Death receptors: signaling and modulation. Science (Wash. DC) 1998;281:1305–8.

13. Datta R, Banach D, Kojima H, et al. Activation of CPP32 protease in apoptosis induced by 1-β-D-arabinofuranosylcytosine and other DNA-damaging agents. Blood 1996;88:1936–43.

14. Friesen C, Herr I, Krammer PH, Debatin KM. Involvement of the CD95 (APO-1/FAS) receptor/ligand system in drug-induced apoptosis in leukemia cells. Nat Med 1996;2:574–7.

15. Marchetti P, Castedo M, Susin SA, et al. Mitochondrial permeability transition is a central coordinating event of apoptosis Bcl-2 inhibits the mitochondrial release of an apoptotic protease. J Exp Med 1996; 184:1155–60.

16. Du C, Fand M, Li Y, Li L, Wang X. Smac, a mitochondrial protein that promotes cytochrome c-dependent caspase activation by eliminating IAP inhibition. Cell 2000;102:33–42.

17. Verphagen AM, Ekert PG, Pakusch M, et al. Identification of DIABLO, a mammalian protein that promotes apoptosis by binding to and antagonizing IAP proteins. Cell 2000;102:43–53.

18. Hengartner MO. The biochemistry of apoptosis. Nature (Lond.) 2000;407:770–6.

19. Li H, Zhu H, Xu CJ, Yuan J. Cleavage of BID by caspase 8 mediates the mitochondrial damage in the Fas pathway of apoptosis. Cell 1998;94:491–501.

20. Lanotte M, Martin-Thouvenin V, Njiman S, et al. NB4, a maturation inducible cell line with t(15;17) marker isolated from a human acute promyelocytic leukemia (M3). Blood 1991;77:1080–6.

21. Kizaki M, Matsushita H, Takayama N, et al. Esablishment and characterization of a novel acute promyelocytic leukemia cell line (UF-1) with retinoic acid-resistant features. Blood 1996;88:1824–33.

22. Murakami A, Toyota K, Ohura S, Koshimizu K, Ohigashi H. Structure-activity relationships of (1′S)-1′-acetoxychavicol acetate, a major constituent of a Southeast Asia condiment plant Languas galangal, on the inhibition of tumor promoter-induced Epstein-Barr virus activation. J Agric Food Chem 2000;48:1518–23.

23. Fukuchi Y, Kizaki M, Kinjo K, et al. Establishment of a retinoic acid resistant acute promyelocytic leukemia model in hGM-CSF transgenic SCID mice. Br J Cancer 1998;78:878–84.

24. Workman P, Balman A, Hickman JA, et al. UKCCCR guidelines for the welfare of animals in experimental neoplasia. Br J Cancer 1998;58:109–13.

25. Mann J. Natural products in cancer chemotherapy: past, present and future. Nat Rev Cancer 2002;2:143–8.

26. Green DR, Reed JC. Mitochondria and apoptosis. Science (Wash. DC) 1998;281:1309–12.

27. Zang L, Yu L, Park BH, Kinzler KW, Vogelstein B. Role of Bax in the apoptotic response to anticancer agent. Science (Wash. DC) 2000; 290:989–92.

28. Park MT, Kang JA, Choi JA, et al. Phytosphingosine induces apoptotic cell death via caspase 8 activation and Bax translocation in human cancer cells. Clin Cancer Res 2003;9:878–85.

29. Li P, Nijhawan D, Budihardjo I, et al. Cytochrome c and d ATP-dependent formation of Apaf-1/caspase-9 complex initiates an apoptotic protease cascade. Cell 1997;91:479–89.

30. Troyano A, Fernandez C, Sancho P, de Blas E, Aller P. Effect of glutathione depletion on antitumor drug toxicity (apoptosis and necrosis) in U937 human promyelocytic cells. J Biol Chem 2001;276:47107–15.

31. Albina JE, Cui S, Mateo RB, Reichner JS. Nitric oxide-mediated apoptosis in murine peritoneal macrophages. J Immunol 1993;150: 5080–5.

32. Pervaiz S, Ramalingam JK, Hirpara JL, Clement M. Superoxide anion inhibits drug-induced tumor cell death. FEBS Lett 1999;459: 343–8.

33. Huang P, Feng P, Oldham EA, Keating MJ, Plunkett W. Superoxide dismutases as a target for the sensitive killing of cancer cells. Nature (Lond.) 2000;407:390–5.

34. Dai J, Weinberg RS, Waxman S, Jing Y. Malignant cells can be sensitized to undergo growth inhibition and apoptosis by arsenic trioxide through modulation of the glutathione redox system. Blood 1999;93: 268–77.

35. Jing Y, Dai J, Chalmens-Redman RME, Tatton WG, Waxman S. Arsenic trioxide selectively induces acute promyelocytic leukemia cell apoptosis via a hydrogen peroxide-dependent pathway. Blood 1999;94: 2102–11.

36. Deveraux QL, Roy N, Stennicke HR, et al. IAPs blocks apoptotic events induced by caspase-8 and cytochrome c by direct inhibition of distinct caspases. EMBO J 1998;17:2215–23.

37. Kluck RM, Bossy-Wetzel E, Green DR, Newmeyer DD. The release of cytochrome c from mitochondria: a primary site for Bcl-2 regulation of apoptosis. Science (Wash. DC) 1997;275:1132–6.

38. Zinkel SS, Ong CC, Ferguson DO, et al. Proapoptotic Bid is required for myeloid homeostasis and tumor suppression. Genes Dev 2003;17:229–39.

39. Gajate C, An F, Mollinedo F. Rapid and selective apoptosis in human leukemic cells induced by aplidine through a Fas/CD95- and mitochondrial-mediated mechanism. Clin Cancer Res 2003;9:1535–45.

40. Minana JB, Gomez-Cambronero L, Lloret A, et al. Mitochondrial oxidative stress and CD95 ligand: a dual mechanism for hepatocyte apoptosis in chronic alcoholism. Hepatology 2002;35:1205–14.

41. Ogasawara J, Watanabe-Fukunaga R, Adachi M, et al. Lethal effect of the anti-Fas antibody in mice. Nature (Lond.) 1993;364:806–9.

[CANCER RESEARCH 64, 1071–1078, February 1, 2004]

# Induction of Apoptosis in Leukemic Cells by Homovanillic Acid Derivative, Capsaicin, through Oxidative Stress: Implication of Phosphorylation of p53 at Ser-15 Residue by Reactive Oxygen Species

**Keisuke Ito,[1] Tomonori Nakazato,[1] Kenji Yamato,[4] Yoshitaka Miyakawa,[1] Taketo Yamada,[2] Nobumichi Hozumi,[5] Kaoru Segawa,[3] Yasuo Ikeda,[1] and Masahiro Kizaki[1]**

*[1]Division of Hematology, Department of Internal Medicine and Departments of [2]Pathology and [3]Microbiology and Immunology, Keio University School of Medicine, Tokyo, Japan; [4]Molecular Cellular Oncology and Microbiology, Graduate School, Tokyo Medical and Dental University, Tokyo, Japan; and [5]Institute of Biological Science, Science University of Tokyo, Chiba, Japan*

## ABSTRACT

**Capsaicin (*N*-vanillyl-8-methyl-1-nonenamide) is a homovanillic acid derivative found in pungent fruits. Several investigators have reported the ability of capsaicin to inhibit events associated with the promotion of cancer. However, the effects of capsaicin on human leukemic cells have never been investigated. We investigated the effects of capsaicin on leukemic cells *in vitro* and *in vivo* and further examined the molecular mechanisms of capsaicin-induced apoptosis in myeloid leukemic cells. Capsaicin suppressed the growth of leukemic cells, but not normal bone marrow mononuclear cells, via induction of $G_0$-$G_1$ phase cell cycle arrest and apoptosis. Capsaicin-induced apoptosis was in association with the elevation of intracellular reactive oxygen species production. Interestingly, capsaicin-sensitive leukemic cells were possessed of wild-type p53, resulting in the phosphorylation of p53 at the Ser-15 residue by the treatment of capsaicin. Abrogation of p53 expression by the antisense oligonucleotides significantly attenuated capsaicin-induced cell cycle arrest and apoptosis. Pretreatment with the antioxidant *N*-acetyl-L-cystein and catalase, but not superoxide dismutase, completely inhibited capsaicin-induced apoptosis by inhibiting phosphorylation of Ser-15 residue of p53. Moreover, capsaicin effectively inhibited tumor growth and induced apoptosis *in vivo* using NOD/SCID mice with no toxic effects. We conclude that capsaicin has potential as a novel therapeutic agent for the treatment of leukemia.**

## INTRODUCTION

Capsaicin is the active principle ingredient of the hot chilli pepper Capsicum, which contains about 0.1–1.0% of capsaicin (1). Spicy foods may play some role in human carcinogenesis, and to date one single epidemiological study has demonstrated that there was a correlation between hot chilli pepper consumption and incidence of gastric cancer (2); however, other studies have failed to provide evidence for its genotoxic potential (3, 4). Capsaicin extracts have been extensively investigated for their effects on genotoxicity and mutagenicity *in vitro* as well as *in vivo*, but the study results are conflicting (5–7). In several studies, the tumor-initiating or -promoting potential of capsaicin was observed (8–11), whereas in other studies the chemoprotective effects of capsaicin were demonstrated (5, 12–14). Moreover, it has been reported that capsaicin inhibits cellular growth of neuroblastoma and hepatocarcinoma cells through the induction of apoptosis (15–17). However, the mechanism of capsaicin-induced apoptosis remains unclear, and the effects of capsaicin on human leukemic cells have never been studied.

Received 6/11/03; revised 10/22/03; accepted 11/06/03.

Grant support: In part by the Ministry of Education, Culture, Sports, Science, and Technology of Japan and by the Keio University Medical Science Fund from Keio University, Tokyo, Japan

The costs of publication of this article were defrayed in part by the payment of page charges. This article must therefore be hereby marked *advertisement* in accordance with 18 U.S.C. Section 1734 solely to indicate this fact.

Requests for reprints: Masahiro Kizaki, Division of Hematology, Department of Internal Medicine, Keio University School of Medicine, 35 Shinanomachi, Shinjuku-ku, Tokyo 160-8582, Japan. Phone: 81-3-5363-3785; Fax: 81-3-3353-3515; E-mail: makizaki@sc.itc.keio.ac.jp.

The tumor suppressor protein p53 regulates the cellular response to DNA damage by mediating cell cycle arrest, DNA repair, and cell death (18, 19). The mechanisms involved in p53-mediated cell death remain controversial, and regulation of p53 function is complicated. Phosphorylation at the Ser-15 residue of p53 is critical for p53-dependent transactivation. In addition, accumulation of p53 protein by inhibiting the interaction between p53 and MDM2 stimulates p53-dependent transactivation (20). In response to stress signals, levels of p53 protein are rapidly increased, and its activity is enhanced after phosphorylation at the Ser-15 residue, resulting in the up-regulation of downstream genes, including the cyclin-dependent kinase inhibitor $p21^{WAF1/CIP1}$ and the proapoptotic gene *Bax*. In turn, increased levels of Bax induce mitochondrial depolarization, release of cytochrome *c*, and activation of a caspase cascade, leading to apoptosis (9, 21–25). Ataxia telangiectasia mutated kinase has been shown to phosphorylate the Ser-15 residue of p53, leading to apoptotic signal transduction (26, 27). Several studies have demonstrated that reactive oxygen species (ROS) generation phosphorylates and activates p53 in an ataxia telangiectasia mutated-dependent manner (28–32).

In the present study, we show that the homovanillic acid derivative capsaicin inhibits the proliferation of various leukemic cells. Capsaicin dramatically suppressed the growth of leukemic cells with wild-type p53, through the induction of $G_0$-$G_1$ cell cycle arrest and apoptosis. We further investigated the molecular mechanisms of capsaicin-induced apoptosis in leukemic cells *in vitro* as well as its antitumor effects *in vivo*.

## MATERIALS AND METHODS

**Cell Culture.** NB4 promyelocytic leukemia and Kasumi-1 myeloid leukemia cell lines were generous gifts from Dr. M. Lanotte (Hôpital St. Louis, Paris, France; Ref. 33) and Dr. H. Asou (Hiroshima University, Hiroshima, Japan; Ref. 34), respectively. Retinoic acid-resistant acute promyelocytic leukemia cell line UF-1 was established in our laboratory (35). The human leukemic cell lines, including HL-60, K562, KU812, and U937, and NIH3T3 cells as a positive control for wild-type p53, were obtained from the Japan Cancer Research Resources Bank (Tokyo, Japan). Bone marrow samples from eight patients with acute leukemia and three normal volunteers were obtained according to appropriate Human Protection Committee validation at the Keio University School of Medicine (Tokyo, Japan) with written informed consent. Mononuclear cells were separated by Lymphoprep (Nycomed Pharma As, Oslo, Norway). Cells were maintained in RPMI 1640 (Life Technologies, Inc., Grand Island, NY) with 10% fetal bovine serum (Life Technologies, Inc.), 100 units/ml penicillin, and 100 μg/ml streptomycin in a humidified atmosphere with 5% $CO_2$. UF-1 and primary cells from the patients were grown in RPMI 1640 with 15% fetal bovine serum (Hyclone Laboratories, Logan, MT) under standard culture conditions. The morphology was evaluated by cytospin slide preparation with Giemsa staining, and the viability was assessed by trypan blue dye exclusion.

**Reagents.** Capsaicin was purchased from Sigma (St. Louis, MO) and dissolved in 100% ethanol, and *N*-tert-butoxy-carbonyl-Val-Ala-Asp-fluoromethylketone (Calbiochem, La Jolla, CA) was dissolved in DMSO (Sigma).

NAC, buthionine sulfoximine, catalase, and superoxide dismutase were purchased from Sigma.

**Cell Cycle Analysis.** Cells ($1 \times 10^6$) were suspended in hypotonic solution (0.1% Triton X-100, 1 mM Tris-HCl (pH 8.0), 3.4 mM sodium citrate, and 0.1 mM EDTA) and stained with 50 $\mu$g/ml of propidium iodide. DNA content was analyzed by FACSCalibur (Becton Dickinson, San Jose, CA). The population of cells in each cell cycle phase was determined using Cell ModiFIT software (Becton Dickinson).

**Assays for Apoptosis.** Apoptotic cells were quantified by Annexin V-FITC and propidium iodide double staining using a staining kit from PharMingen (San Diego, CA). The mitochondrial transmembrane potential ($\Delta\psi m$) was determined by flow cytometry. Briefly, cells were washed twice with PBS and incubated with 1 $\mu$g/ml Rhodamine 123 (Sigma) at 37°C for 30 min. Rhodamine 123 intensity was determined by flow cytometry.

**Caspase Assays.** Caspase-3-related protease activity was determined by using a commercially available kit (PharMingen) according to the manufacturer's instructions. Briefly, cells were fixed and permeabilized using the Cytofix/Cytoperm for 20 min at 4°C, pelleted, and washed with Perm/Wash buffer (PharMingen). Cells were then stained with polyclonal antibody against the active form of caspase-3 (PharMingen) for 20 min at room temperature, washed in Perm/Wash buffer, stained with goat antirabbit-FITC (Super Techs, Bethesda, MD), and analyzed by flow cytometry. In the caspase inhibitor assay, cells were pretreated with a synthetic pan-caspase inhibitor (20 $\mu$M; *N*-tert-butoxy-carbonyl-Val-Ala-Asp-fluoromethylketone) for an hour before addition of capsaicin.

**Measurement of ROS Production.** To assess the generation of ROS, we incubated control and capsaicin-treated cells with 5 $\mu$M dihydroethidium (Molecular Probes, Eugene, OR), which is rapidly oxidized to the fluorescent intercalator ethidium by cellular oxidants. Cells ($1 \times 10^5$) were stained with 5 $\mu$M dihydroethidium for 15 min at 37°C and were then washed and resuspended in PBS. The oxidative conversion of dihydroethidium to ethidium was analyzed by flow cytometry.

**Cell Lysate Preparation and Immunoblotting.** Cells were collected by centrifugation at 700 × *g* for 10 min, and then the pellets were resuspended in a lysis buffer [1% NP40, 1 mM phenyomethylsulfonyl fluoride, 40 mM Tris-HCl (pH 8.0), and 150 mM NaCl] at 4°C for 15 min. Mitochondrial and cytosolic fractions were prepared with digitonin-nagarse treatment. Protein concentrations were determined using a detergent-compatible protein assay system (Bio-Rad, Richmond, CA). Cell lysates (15 $\mu$g of protein/lane) were fractionated in 12.5% or 7.5% SDS-polyacrylamide gels before being transferred to the membrane (Immobilon-P membrane; Millipore, Bedford, MA) according to standard protocol. Antibody binding was detected by using the enhanced chemiluminescence kit with hyper-enhanced chemiluminescence film (Amersham, Buckinghamshire, United Kingdom). $\beta$-Actin was used as an indicator for equality of lane loading. Blots were also stained with Coomassie Brilliant Blue to confirm that equal amounts of protein extracts were present in each lane. The following antibodies were used in this study: anti-Rb, -cytochrome *c* (PharMingen), -MDM2 (Oncogene, Boston, MA), -p53, -phospho Rb (Ser-780; Cell Signaling, Beverly, MA), -cyclin D1, -Bax, -$p21^{WAF1/CIP1}$, and -$\beta$-actin (Santa Cruz Biotechnology, Santa Cruz, CA). We used p53-phosphorylated kit (Cell Signaling) to detect phosphorylated p53. For detection of wild-type p53 protein expression, cell lysates were precipitated with anti-p53 wild-type monoclonal antibody (PAb1620; Oncogene) and then blotted with anti-p53 polyclonal antibody (Cell Signaling). Expression of wild-type p53 was also determined by flow cytometry.

**Reverse Transcription-PCR, PCR, Gel Electrophoresis, and Sequencing.** Total cellular RNAs were isolated from the cells by using RNA easy kit (Qiagen K.K., Tokyo, Japan). Random primed, first strand cDNAs were synthesized from 1 $\mu$g of total RNAs using Superscript II reverse transcriptase (Life Technologies, Inc. Gaithersburg, MD) according to the manufacturer's instructions. PCR was carried out for 30 s at 94°C, 30 s at 55°C, and 20 s at 72°C for 40 cycles. Primer sequences for p53 were sense (nucleotide 225-244) 5′-TGCACCAGCGACTCCTACAC-3′ and antisense (nucleotide 892-873) 5′-CTGGGTGAGGCTCCCCTTTC-3′. The PCR products were analyzed on 1% agarose gel. To normalize the amount of RNA, we used amplification of the human $\beta$-actin gene as a control. Exons 4-11 of the "hot spots" region of p53 were amplified by PCR using the following primers: 5′-GCCAAGTCTGT-GACCTGCACG-3′ (exon 4) and 5′-TCAGTCTGAGTCAGGCCCTTC-3′ (exon 11). The amplified product was cloned into a pCR2.1 TOPO vector (Invitrogen, Carlsbad, CA) and sequenced with both M13 forward primer and M13 reverse primer included in the TOPO TA cloning kit (Invitrogen) according to the manufacturer's recommendation. DNA sequencing was performed on an ABI PRISM 310 genetic analyzer (Perkin-Elmer Applied Biosystems, Foster City, CA). All of the oligonucleotides were obtained from Sawaday Technology (Tokyo, Japan).

**Antisense Oligonucleotides for p53.** The p53-antisense oligodeoxynucleotide targeted the following region of the initiation codon: 5′-CGGCTCCTC-CATGGCAGT-3′. Its scrambled oligodeoxynucleotide (5′-ACTGCCATG-GAGGAGCCG-3′) and the mismatch sequence (5′-CGGGTCCTCTACG-CTAGT-3′) were designed as a negative control. These oligodeoxynucleotides were modified by phosphorothioate to enhance their stability, and they had no similarity to other mammalian genes as shown by Basic Local Alignment Search Tool search analysis. After 24 h of preincubation with these oligonucleotides, NB4 cells were treated with capsaicin and 1 $\mu$M each oligonucleotide for 24 h.

**Animal Model and Experimental Design.** We have established a system of human all-*trans* retinoic acid-sensitive acute promyelocytic leukemia model in NOD/SCID mice by using NB4 cells (36). Briefly, NOD/SCID mice (The Jackson Laboratory, Bar Harbor, ME) were pretreated with 3 Gy of total body irradiation, which is a sublethal dose that was expected to enhance the acceptance of xenografts. Subsequently, the mice were inoculated s.c. with NB4 cells ($1 \times 10^7$ cells) in their logarithmic growth phase, and the inoculated NB4 cells rapidly formed s.c. tumors at the injection site. Fourteen days after implantation of the cells, mice with the transplanted cells were randomly assigned to be injected with 5% ethanol ($n = 15$; 50 $\mu$l) or capsaicin (50 mg/kg) in 5% ethanol ($n = 15$; 50 $\mu$l) as an emulsion fluid administered daily. After 6 days of the treatment, mice were sacrificed and dissected to measure tumor weights. The study was approved by the Animal Care and Use Committee at the Keio University School of Medicine, Tokyo, Japan. When the mice showed severe wasting or when observations were finished, mice were sacrificed according to the UKCCCR guidelines (37). Tumors were fixed in 4% paraformaldehyde, embedded in paraffin, sectioned, and then stained with anti-single-strand DNA (Dako Japan Co., Ltd, Kyoto, Japan) for detection of apoptotic cells (38).

**Statistical Analysis.** Tumor weights and numbers of mitotic cells are expressed as the mean ± SD. Differences of both parameters were analyzed for significance by Student's *t* test. $P < 0.05$ was considered to indicate statistical significance.

## RESULTS

**Effects of Capsaicin on Cellular Proliferation of Various Leukemic Cells.** We first investigated the effects of capsaicin on cellular proliferation of seven leukemic cell lines that included NB4, UF-1, Kasumi-1, HL-60, K562, KU812, and U937 cells. Capsaicin inhibited cellular growth of all leukemic cells, but not normal bone marrow mononuclear cells, in a dose- and time-dependent manner (Fig. 1, *A* and *B*). Interestingly, capsaicin was particularly sensitive to NB4 and Kasumi-1 leukemic cells (Fig. 1, *A* and *B*), both of which expressed PAb1620-reactive wild-type p53 (Fig. 2, *A* and *B*). In addition, sequencing analysis of p53 (exons 4-11) was performed on both cell lines that have wild-type p53 (data not shown). But the other leukemic cell lines had defective p53 (Fig. 2, *A* and *B*). As previous investigations have reported, these cell lines contain mutated p53 alleles (39–42). Because capsaicin dramatically decreased cellular growth of NB4 and Kasumi-1 cells with the lowest $IC_{50}$, we used NB4 cells for our subsequent investigations. Cultivation with capsaicin increased the population of cells in the $G_0$-$G_1$ phase with a reduction of cells in the S-phase, which was followed by a marked increase of a sub-$G_1$ population at 24 h (Fig. 1*C*). Annexin V-positive apoptotic fractions were detected beginning 4 h after exposure to capsaicin, and these fractions dramatically increased in a time-dependent manner (Fig. 1*D*). Annexin V and propidium iodide double-positive cells were increased at 24 h after treatment, indicating that capsaicin induced